MOLECULAR AND CELLULAR BIOLOGY, May 1998, p. 2697–2711 Vol. 18, No. 5
0270-7306/98/$04.00+0
Copyright © 1998, American Society for Microbiology

Dimerization by Translation Initiation Factor 2 Kinase GCN2 Is Mediated by Interactions in the C-Terminal Ribosome-Binding Region and the Protein Kinase Domain

HONGFANG QIU, MINERVA T. GARCIA-BARRIO, AND ALAN G. HINNEBUSCH*

Laboratory of Eukaryotic Gene Regulation, National Institute of Child Health and Human Development, Bethesda, Maryland 20892

Received 21 November 1997/Returned for modification 5 January 1998/Accepted 2 February 1998

The protein kinase GCN2 stimulates translation of the transcriptional activator *GCN4* in yeast cells starved for amino acids by phosphorylating translation initiation factor 2. Several regulatory domains, including a pseudokinase domain, a histidyl-tRNA synthetase (HisRS)-related region, and a C-terminal (C-term) segment required for ribosome association, have been identified in GCN2. We used the yeast two-hybrid assay, coimmunoprecipitation analysis, and in vitro binding assays to investigate physical interactions between the different functional domains of GCN2. A segment containing about two thirds of the protein kinase (PK) catalytic domain and another containing the C-term region of GCN2 interacted with themselves in the two-hybrid assay, and both the PK and the C-term domains could be coimmunoprecipitated with wild-type GCN2 from yeast cell extracts. In addition, in vitro-translated PK and C-term segments showed specific binding in vitro to recombinant glutathione *S*-transferase (GST)–PK and GST–C-term fusion proteins, respectively. Wild-type GCN2 could be coimmunoprecipitated with a full-length LexA-GCN2 fusion protein from cell extracts, providing direct evidence for dimerization by full-length GCN2 molecules. Deleting the C-term or PK segments abolished or reduced, respectively, the yield of GCN2–LexA-GCN2 complexes. These results provide in vivo and in vitro evidence that GCN2 dimerizes through self-interactions involving the C-term and PK domains. The PK domain showed pairwise in vitro binding interactions with the pseudokinase, HisRS, and C-term domains; additionally, the HisRS domain interacted with the C-term region. We propose that physical interactions between the PK domain and its flanking regulatory regions and dimerization through the PK and C-term domains both play important roles in restricting GCN2 kinase activity to amino acid-starved cells.

The protein kinases that phosphorylate the α subunit of eukaryotic translation initiation factor 2 (eIF2α) on serine-51 down-regulate protein synthesis in response to starvation or stress. In both mammalian and yeast cells, phosphorylation of eukaryotic translation initiation factor 2 (eIF2) converts it from a substrate to an inhibitor of its guanine nucleotide exchange factor, eIF2B, decreasing the recycling of eIF2 from the GDP-bound to the GTP-bound state. Only the GTP-bound form of eIF2 is competent to form a ternary complex with charged initiator $tRNA^{Met}$ and interact with the 43S preinitiation complex; thus, phosphorylation of eIF2 impairs a key step in translation initiation (14, 22). The mammalian eIF2α kinase HRI is activated in erythroid cells by hemin deficiency as a means of reducing globin synthesis when hemin is limiting. The eIF2α kinase PKR is thought to be activated in virus-infected mammalian cells, where it inhibits total protein synthesis by phosphorylation of eIF2 and thereby limits virus proliferation (21).

The eIF2α kinase of *Saccharomyces cerevisiae*, known as GCN2, becomes activated in response to starvation for one or more amino acids and specifically induces the translation of *GCN4* mRNA, encoding a transcriptional activator of amino acid biosynthetic genes. The newly synthesized GCN4 protein derepresses numerous amino acid biosynthetic enzymes, alleviating the amino acid starvation that triggered its induction. Four short upstream open reading frames (uORFs) in the leader of *GCN4* mRNA cause its translation to be inversely coupled to the levels of eIF2–GTP–Met-$tRNA_i^{Met}$ ternary complexes in the cell. Under nonstarvation conditions, where ternary complexes are plentiful, ribosomes scanning from the 5′ end of *GCN4* mRNA translate the uORFs and fail to reinitiate at the *GCN4* start codon downstream. When ternary complex levels are decreased by phosphorylation of eIF2 in starved cells, ribosomes bypass the inhibitory uORFs and initiate translation at *GCN4* instead (15, 16).

Mutations that lead to constitutive activation of kinase function in the absence of amino acid starvation have been isolated in *GCN2*. Some of these *GCN2*^{c} alleles confer such high levels of eIF2α phosphorylation in vivo that general translation initiation is inhibited and cell growth is impaired (7, 25, 32). Because GCN2 is expressed constitutively (32) and its activation has the potential to arrest cell growth, the activity of the protein kinase (PK) domain must be tightly regulated to restrict its function to starvation conditions, where GCN4 is induced. GCN2 is a large protein (≈190 kDa) containing multiple regulatory domains that are required to couple its eIF2α kinase activity to the levels of amino acids in the cell (32).

Uncharged tRNA appears to be the activating ligand for GCN2 because mutations in aminoacyl-tRNA synthetases lead to increased eIF2α phosphorylation by GCN2 (33), with attendant derepression of *GCN4* (18) and genes under its control (23, 30, 33). GCN2 contains a C-terminal (C-term) regulatory domain similar in sequence to histidyl-tRNA synthetase (HisRS) (5, 31), and it is thought that binding of uncharged tRNA to this HisRS domain produces in the adjacent kinase domain a conformational change that increases its ability to

* Corresponding author. Mailing address: Laboratory of Eukaryotic Gene Regulation, National Institute of Child Health and Human Development, Building 6A, Room B1A-13A, Bethesda, MD 20892-2716. Phone: (301) 496-4480. Fax: (301) 496-6828. E-mail: ahinnebusch@nih.gov.

phosphorylate eIF2 (31). In support of this model, it was shown that a conserved sequence characteristic of authentic class II aminoacyl-tRNA synthetases (motif 2) found in the HisRS domain of GCN2 is required for kinase function in vivo and in vitro as well as for binding of uncharged yeast tRNA to the HisRS domain of GCN2 in vitro (33, 35). In addition, numerous *GCN2*^{c} activating mutations alter residues in the HisRS region, including two conserved positions in motif 2 (7, 25, 32).

There is biochemical evidence that GCN2 can interact with translating ribosomes and free ribosomal subunits and that this association is dependent on the C-term 120 amino acids of the protein (24). The C-term domain is required for *GCN2* function in vivo (24), leading to the suggestion that GCN2 is activated by uncharged tRNA bound to ribosomes during translation elongation (25). Interestingly, the *GCN2*^{c} alleles which activate GCN2 most effectively alter residues in the C-term domain (7, 25, 32); thus, this segment may function both in anchoring GCN2 to the ribosome and in facilitating activation of the kinase domain by uncharged tRNA. In addition to the HisRS and C-term segments, GCN2 contains a regulatory domain N terminal to the kinase moiety that is required in vivo (32) and in vitro (35) for kinase activity. This region contains sequence similarity to multiple subdomains of eukaryotic protein kinases, although critical residues in putative subdomains I, II, and VI important for ATP binding and catalysis appear to be lacking (12, 31). The function of this degenerate kinase domain, referred to here as the pseudokinase (ψPK) domain, in regulating the authentic PK domain of GCN2 is unknown.

There is limited genetic and biochemical evidence that the dimerization of GCN2 is important for its activation or catalytic function. The *GCN2*^{c}*-E1525K* allele encodes a hyperactive kinase that inhibits translation initiation so severely that cell growth is impaired. This slow-growth phenotype was suppressed by coexpression of wild-type *GCN2* (7), and similar observations have been made for other *GCN2*^{c} alleles (8a). To account for this phenomenon, it was proposed that the hyperactive mutant and wild-type GCN2 proteins form oligomers that are less active for eIF2 phosphorylation than oligomers containing only GCN2^c proteins. In addition, much of the GCN2 protein eluted from a sizing column with apparent molecular masses much larger than the mass of monomeric GCN2 (7). It is also noteworthy that the HisRS domain of GCN2 contains a relatively good match to sequence motif I, which contributes to dimer formation in class II aminoacyl-tRNA synthetases (5). It was suggested that a GCN2 homodimer might bind to a single tRNA molecule and that intermolecular autophosphorylation by the two GCN2 protomers would activate the eIF2α kinase function (7).

We present here genetic and biochemical evidence that GCN2 contains at least two domains that mediate dimerization, the PK domain and the C-term ribosome-binding domain, and show that the latter is more critically required for self-interaction by full-length GCN2 molecules in vivo. We also detected independent interactions between the C-term region and the PK and HisRS domains and found that the PK domain interacts strongly with the HisRS and ψPK domains. Our observations suggest that the regulation of GCN2 kinase activity involves both protein dimerization and physical interactions between the kinase domain and each of its flanking regulatory regions.

MATERIALS AND METHODS

Yeast strains and plasmids. EGY48 (*MAT*α *trp1 ura3 his3 lexAop-LEU2*) (11) was used for all two-hybrid interaction assays. HQY132, a *gcn2*Δ derivative of EGY48, was used for all coimmunoprecipitation experiments and glutathione *S*-transferase (GST)-binding assays in which yeast extracts were the source of LexA-GCN2 fusions and was constructed as follows. A 3.8-kb *hisG::URA3::hisG* fragment was inserted at the *Bgl*II site of plasmid p1141 (a gift from T. Dever), from which the *GCN2* open reading frame was deleted, to produce plasmid pHQ414, bearing a *gcn2*Δ *hisG::URA3::hisG* allele. pHQ414 was digested with *Eco*RI and *Xba*I, and the *Eco*RI-*Xba*I fragment containing *gcn2*Δ *hisG::URA3::hisG* was used to transform EGY48 to Ura$^+$. The deletion of *GCN2* in the resulting transformants was confirmed by PCR with a pair of primers complementary to the sequence of the *GCN2* promoter region (that was not deleted) and *URA3*. Finally, strain HQY132 was obtained by selecting for loss of the *URA3* marker via homologous recombination between the *hisG* repeats on medium containing 5-fluoro-orotic acid (2). Strain H1613 was described previously (25).

Plasmids pEG202 and pJG4-5 (10) were used for constructing plasmids expressing LexA and B42 activation domain fusions, respectively. pSH18-34 contains the *lexAop-lacZ* reporter, and pRFHM1 contains LexA fused to the homeodomain of *Drosophila* bicoid (10). For constructing plasmids expressing LexA or B42 fusions bearing GCN2 amino acid residues 230 to 604 (pHQ385 and pHQ435), 720 to 999 (pHQ433 and pHQ428), 750 to 999 (pHQ425 and pHQ429), 970 to 1497 (pHQ426 and pHQ430), 1080 to 1497 (pHQ434 and pHQ431), and 1150 to 1497 (pHQ432), DNA fragments encoding the appropriate GCN2 segments were synthesized by PCR, adding *Eco*RI and *Xho*I (or *Sal*I for the segment encoding residues 720 to 999) sites at their 5′ and 3′ ends, respectively. The resulting fragments were inserted in frame between the *Eco*RI and *Xho*I sites of pEG202 (or p2247 to construct pHQ385) and pJG4-5. Plasmid pHQ311, encoding LexA-GCN2(1498-1659) (bearing GCN2 residues 1498 to 1659), was created by inserting an ~0.78-kb *Bcl*I fragment from p585 containing wild-type *GCN2* (32) at the *Bam*HI site of pEG202. An 0.8-kb *Eco*RI-*Xho*I fragment from pHQ311 was then inserted into pJG4-5 at the *Eco*RI and *Xho*I sites to produce plasmid pHQ314. Plasmid pHQ316, encoding B42-GCN2(82-551), was constructed in two steps. First, an ~0.56-kb *Hpa*I fragment from p585 was inserted at the filled-in *Xho*I site of pJG4-5 to produce plasmid pHQ310; the *Eco*RI fragment of pHQ310 was replaced with the *Eco*RI fragment of *GCN2* from p585 to produce plasmid pHQ316. Plasmid pHQ400, encoding nearly full-length GCN2 fused to LexA [LexA-hemagglutinin (HA)-GCN2(27-1659)], was constructed by inserting the PCR-synthesized *Bam*HI-*Asp*718 fragment and the *Asp*718-*Sal*I fragment from plasmid pC102-2 (a YCp50-based *GCN2* plasmid) (8) between the *Bam*HI and *Sal*I sites of plasmid p2247, containing the coding sequences for two copies of the HA epitope upstream of the *Eco*RI site in pEG202 (34).

Plasmid pHQ325, encoding LexA-GCN2(1498-1659)-1571SS (a Ser-Ser insertion at GCN2 amino acid 1571), was created by inserting the ~0.77-kb *Bcl*I-*Sal*I fragment from p558 bearing the *gcn2-1571SS* allele (31) into pEG202 at the *Bam*HI and *Sal*I sites. An ~0.78-kb *Eco*RI-*Sal*I fragment from pHQ325 was inserted into pJG4-5 at the *Eco*RI and *Xho*I sites to produce pHQ331, encoding B42-GCN2(1498-1659)-1571SS. An ~0.78-kb *Bcl*I fragment from p915 bearing the *GCN2*^{c}*-E1591K* allele (25) was cloned into pEG202 at the *Bam*HI site to produce pHQ327, encoding LexA-GCN2(1498-1659)-E1591K, and the *Eco*RI-*Xho*I fragment from pHQ327 was cloned into pJG4-5 to produce pHQ330, encoding B42-GCN2(1498-1659)-E1591K. pHQ356, encoding LexA-GCN2(1498-1659)-1656EL, and pHQ362, encoding B42-GCN2(1498-1659)-1656EL, as well as pHQ354, encoding LexA-GCN2(1498-1659)-1536SS, and pHQ361, encoding B42-GCN2(1498-1659)-1536SS, were constructed by inserting ~0.77-kb *Bcl*I-*Sal*I fragments from p563 and p560 (32) into pEG202 and pHQ346 at the *Bam*HI and *Sal*I sites, respectively. pHQ346 is a derivative of pJG4-5 with the same cloning sites as pEG202 and was constructed by replacing an ~0.5-kb *Eco*RI-*Not*I fragment of pJG4-5 containing the ADH1 terminator with an *Eco*RI-*Eag*I PCR fragment containing multiple cloning sites and the ADH1 terminator synthesized from pEG202.

To construct 5′ and 3′ deletions in the C-term coding region of GCN2 for fusing with LexA and B42, DNA fragments encoding the appropriate GCN2 segments with *Eco*RI and *Xho*I sites introduced at their 5′ and 3′ ends, respectively, were synthesized by PCR and inserted between the *Eco*RI and *Xho*I sites of pEG202 and pJG4-5 to produce plasmids encoding LexA- and B42-GCN2 (1518-1659) (pHQ347 and pHQ337, Δ1498-1517), LexA- and B42-GCN2(1536-1659) (pHQ348 and pHQ338, Δ1498-1535), LexA- and B42-GCN2(1556-1659) (pHQ349 and pHQ339, Δ1498-1555), LexA- and B42-GCN2(1576-1659) (pHQ350 and pHQ340, Δ1498-1575), LexA- and B42-GCN2(1498-1634) (pHQ351 and pHQ341, Δ1635-1659), LexA- and B42-GCN2(1498-1609) (pHQ352 and pHQ342, Δ1610-1659), and LexA- and B42-GCN2(1498-1584) (pHQ353 and pHQ343, Δ1585-1659). (In the foregoing constructs, the numbers following the Δ symbol indicate the GCN2 residues that were deleted.)

For constructing the internal deletions in the C-term coding region of *GCN2*, the 0.95-kb *Pvu*II-*Bst*EII fragment from p585 was inserted at the *Pvu*II site of pUC19 to produce plasmid pHQ368. For each deletion, a pair of primers that contained a *Sac*I site at their 5′ ends and were complementary to the sequences immediately upstream or downstream of the deletion junction on opposite strands was synthesized. These primers were used in PCR with pHQ368 as the template to amplify a linear fragment containing *Sac*I ends. After digestion with *Sac*I, the PCR products were self-ligated to produce the following plasmids with the desired internal deletions and *Sac*I sites at the deletion junctions: pHQ369 (Δ1518-1537), pHQ370 (Δ1538-1557), pHQ371 (Δ1558-1577), pHQ372 (Δ1578-1597), pHQ373 (Δ1598-1617), pHQ374 (Δ1618-1637), pHQ375 (Δ1638-1659), and pHQ387 (Δ1498-1517). From these plasmids (excluding pHQ375 and

TABLE 1. Selected oligonucleotides used for PCR synthesis of DNA fragments encoding segments of GCN2

Primer	Sequence[a]	GCN2 segment encoded (residues)
Forward	230 5′ CCG GGATCC *GCC* **ATG** *G*AC ATG TTC AAG TTT AAA GCA GTT G 3′ *Bam*HI *Nco*I	ψPK (230 to 604)
Reverse	604 5′ CCG CTC GAG **CTA** AAC TGC AAT CTC TTC AAA GTC 3′ *Xho*I	
Forward	970 5′ CGG GAGCTC *GCC* **ATG** *G*AT CCT GGT GCT AGG ACA TTA TTA 3′ *Sac*I *Nco*I *Bam*HI	HisRS (970 to 1497)
Reverse	1497 5′ CCG CTC GAG **CTA** CAA AGA TTT ATT ACC AGT TTC 3′ *Xho*I	
Forward	1498 5′ CGG GGATCC *GCC* **ATG** *G*AT ATC AAC GAT AGT CTC ACT TTG 3′ *Bam*HI *Nco*I *Eco*RV	C-term (1498 to 1659)
Reverse	1659 5′ CCG CTC GAG ATC TTT AAA GGC **CTA** CCT C 3′ *Xho*I *Stu*I	

[a] Numbers above the sequences are the GCN2 residue numbers encoded by the triplets (or the complementary triplets in the case of reverse primers) directly below them. Novel start codons and the complement of stop codons are shown in boldface, and restriction sites recognized by the indicated enzymes are underlined. The italicized sequence surrounding each start codon is the Kozak consensus sequence (16a).

pHQ387), DNA fragments encoding residues 1498 to 1659 were synthesized by PCR with primers introducing *Eco*RI and *Xho*I sites at the 5′ and 3′ ends, respectively, and were inserted between the *Eco*RI and *Xho*I sites of pEG202 and pJG4-5 to produce the following plasmids encoding derivatives of LexA- and B42-GCN2(1498-1659) fusion proteins, respectively, with the indicated deletions: pHQ388 and pHQ394 (Δ1518-1537), pHQ389 and pHQ395 (Δ1538-1557), pHQ390 and pHQ396 (Δ1558-1577), pHQ391 and pHQ397 (Δ1578-1597), pHQ392 and pHQ398 (Δ1598-1617), and pHQ393 and pHQ399 (Δ1618-1637). Plasmid pHQ326, encoding LexA-GCN2(1498-1659)-Δ1536-1570 (lacking residues 1536 to 1570 within the GCN2 segment extending from residues 1498 to 1659), was created by inserting the ~0.67-kb *Bcl*I-*Sal*I fragment from p617 (24) at the *Bam*HI and *Sal*I sites of pEG202. An *Eco*RI-*Sal*I fragment from pHQ326 was cloned into pJG4-5 to produce plasmid pHQ329, encoding B42-GCN2(1498-1659)-Δ1536-1570.

Plasmids bearing full-length *gcn2* alleles, pHQ406 (*gcn2-Δ1498-1517*), pHQ402 (*gcn2-Δ1518-1537*), pHQ407 (*gcn2-Δ1538-1557*), pHQ408 (*gcn2-Δ1558-1577*), pHQ409 (*gcn2-Δ1578-1597*), pHQ403 (*gcn2-Δ1598-1617*), pHQ405 (*gcn2-Δ1618-1637*), and pHQ404 (*gcn2-Δ1638-1659*), were constructed by replacement of the ~0.91-kb *Pvu*II-*Nhe*I fragment of p722 (25) with those derived from pHQ387 (Δ1498-1517), pHQ369 (Δ1518-1537), pHQ370 (Δ1538-1557), pHQ371 (Δ1558-1577), pHQ372 (Δ1578-1597), pHQ373 (Δ1598-1617), pHQ374 (Δ1618-1637), and pHQ375 (Δ1638-1659), respectively.

Plasmid pHQ531, encoding GST–C-term(1498-1659) (bearing GCN2 residues 1498 to 1659), was constructed by inserting the *Eco*RI-*Xho*I fragment encoding GCN2 residues 1498 to 1659 and isolated from pHQ314 into pGEX-5x-1 (Pharmacia) at the *Eco*RI and *Sal*I sites. Plasmid pHQ551, encoding GST-PK(568-998), was created by inserting an ~1.3-kb *Asp*700-*Ecl*136II fragment encoding GCN2 residues 568 to 998 and obtained from p567 into pGEX-5x-2 at the *Sma*I site.

To construct plasmids used for in vitro translation, fragments encoding the appropriate GCN2 segments were synthesized by PCR with primers (Table 1) that introduced restriction sites for cloning purposes and the ATG initiation codon. *Bam*HI- and *Xho*I-digested PCR fragments encoding GCN2 residues 230 to 604 and GCN2 residues 1498 to 1659 were inserted into pGEM-3Z (Promega) between the *Bam*HI and *Sal*I sites to produce pHQ539 and pHQ542, respectively. A *Sac*I- and *Xho*I-digested fragment encoding GCN2 residues 970 to 1497 was inserted into pGEM-3Z between the *Sac*I and *Sal*I sites to produce pHQ541. An ~1.3-kb *Asp*700-*Ecl*136II fragment encoding GCN2 residues 568 to 998 and isolated from p567 was inserted between the *Eco*RV and *Stu*I sites of pHQ542 in place of the *Eco*RV-*Stu*I fragment encoding GCN2 residues 1498 to 1659 to produce pHQ550.

Plasmids used for coimmunoprecipitation experiments were constructed as follows. Plasmids pHQ587, encoding LexA-HA-′PK(720-999) (bearing only a portion of the PK domain from residues 720 to 999), pHQ588, encoding LexA-HA-HisRS(970-1497), and pHQ589, encoding LexA-HA–C-term(1498-1659), were constructed by inserting *Eco*RI-*Sal*I or *Eco*RI-*Xho*I fragments encoding the corresponding GCN2 segments isolated from pHQ428, pHQ430, and pHQ314, respectively, into p2247 (34). Plasmid p2327, carrying a *gcn2-Δ324-538* (ΔψPK) allele, was created by replacing the *Bam*HI fragment of p630, a high-copy-number GCN2 plasmid (32), with the same fragment of p614, carrying the *gcn2-Δ324-538* allele. p614 was created by replacing the *Xba*I-*Sac*I fragment of p568, bearing the *gcn2-538AR* allele (31), with the *Xba*I-*Sac*I fragment of p564, containing *gcn2-324AR* (31). To create plasmid pB82, carrying *gcn2-Δ572-999*, a *Sac*I-*Sal*I fragment of p551 (31) encoding the N terminus of *gcn2-572SS* was ligated with a *Sac*I-*Sal*I fragment of p567 (31) encoding the C terminus of *gcn2-999SS* to produce pB77 containing *gcn2-Δ572-999*. Subsequently, the *Bam*HI fragment of p630 was replaced with the corresponding fragment of pB77 to produce pB82. To create p2463, containing *gcn2-Δ1161-1570*, a *Sac*I-*Sal*I fragment containing the N terminus of *gcn2-Δ1161-1246* from p733 was ligated with a *Sac*I-*Sal*I fragment containing the C terminus of *gcn2-Δ1536-1570* from p734 to produce p774. Plasmid p774 was cut with *Sac*I, and the ends were filled in with Klenow polymerase, followed by ligation to restore the *GCN2* reading frame. Plasmid p2461, containing *gcn2-Δ1536-1659*, was created by replacing the *Asp*718-*Sal*I fragment of p630 with the same fragment of p780. Plasmids p733 and p734 are derivatives of p630 (32) containing internal deletions between *Sac*I insertions described previously (31) at amino acid positions 1161 and 1246 (p733) or 1536 and 1571 (p734). Plasmid p780 was constructed from p560, another derivative of p630 which contains a *Sac*I insertion at position 1536. A pair of complementary oligonucleotides (5′ AATAACTCGAGCAGCT 3′ and 5′ GCTCGAGTTATT AGCT 3′) was annealed and inserted at the *Sac*I site in p560 to introduce a stop codon at position 1536, destroying the *Sac*I site and introducing an *Xho*I site in the process. Plasmid pHQ502 was constructed by PCR amplification of a fragment encoding GCN2 residues 1498 to 1659 with the addition of a 5′ *Sac*I site, ATG codon, and 3′ *Bam*HI site and insertion of this fragment between the *Sac*I and *Bam*HI sites of pEMBLyex4 (4).

Two-hybrid interaction assay. Plasmids encoding the appropriate LexA- and B42-GCN2 fusions were cotransformed into yeast strain EGY48 by use of a modified lithium acetate method (9). The transformants were selected on minimal SD plates (28) supplemented with uracil and leucine (SD+Ura+Leu) and replica printed to SD+Ura and SGal/Raf+Ura media, where the 2% dextrose in SD was replaced with 2% galactose and 1% raffinose in the latter medium. Two-hybrid interactions were indicated by growth on SGal/Raf+Ura but not on SD+Ura plates, indicating a galactose-dependent Leu^+ phenotype. When needed, the *lexAop-lacZ* reporter plasmid pSH18-34 was introduced into transformants carrying *lexA*- and *B42-GCN2* fusion plasmids, and three or more independent transformants were analyzed for β-galactosidase activities in cell extracts. For these assays, cells were grown for ~38 h to saturation in synthetic complete medium lacking uracil, histidine, and tryptophan (SC−Ura−His−Trp) and were diluted 1:50 into the same medium containing galactose (2%) and raffinose (1%) as carbon sources (SC/Gal/Raf−Ura−His−Trp). Cells were harvested in the mid-logarithmic phase after 6 h of growth. β-Galactosidase assays were carried out as described previously (19), and β-galactosidase activities are expressed as nanomoles of *o*-nitrophenyl-β-D-galactopyranoside hydrolyzed per minute per milligram of protein.

Coimmunoprecipitation and immunoblot analysis. For coimmunoprecipitation of wild-type or mutant GCN2 proteins with LexA-GCN2 fusion proteins

from yeast cell extracts, fresh transformants of strain HQY132 bearing the appropriate high-copy-number plasmids encoding the GCN2 and LexA-GCN2 fusion proteins under consideration were grown in SC−Ura−His medium to the exponential phase (optical density at 600 nm, ~1.2 to 1.5). Cells from 20 ml of culture were harvested by centrifugation, washed with ice-cold water, and transferred to a 1.5-ml microcentrifuge tube. Cell pellets were resuspended in 250 μl of breaking buffer (50 mM Tris-HCl [pH 7.5], 50 mM NaCl, 0.1% Triton X-100, 5 μg each of pepstatin A, leupeptin, and aprotinin per ml, 1 mM phenylmethylsulfonyl fluoride, 1 mM dithiothreitol) and broken by vortexing with glass beads, and the extracts were clarified by centrifugation for 15 min in a microcentrifuge. Protein concentrations in the extracts were determined as described previously (3). For immunoprecipitation, 40 μl (10-μl bed volume) of protein A-agarose beads (Santa Cruz) was washed with breaking buffer and resuspended in 200 μl of breaking buffer, after which 10 μg of anti-HA antibody (Boehringer) was added and incubated at room temperature with rocking for 1 h. The beads were collected by brief centrifugation and washed with 500 μl of breaking buffer. Aliquots of cell extracts containing 50 μg of protein were diluted to a final volume of 200 μl with breaking buffer and incubated with 20 μl of protein A-agarose beads suspended in breaking buffer for 1 h at 4°C with rocking. The beads were removed by centrifugation, and the supernatant was added to beads prebound with anti-HA antibody and incubated at 4°C for 2 h with rocking. The beads were collected by centrifugation, washed three times with 500 μl of breaking buffer, and resuspended in 40 μl of Laemmli sample buffer (17). Proteins in the immune complexes were resolved by sodium dodecyl sulfate (SDS)-polyacrylamide gel electrophoresis (PAGE), transferred to nitrocellulose membranes (29), and probed with antibodies against GCN2 or LexA. The immune complexes were visualized by enhanced chemiluminescence (ECL; Amersham) according to the vendor's instructions. Anti-LexA antibodies were a gift from Clyde Denis. Preparation of the anti-GCN2 antibodies will be described elsewhere.

Preparation of GST and GST fusion proteins. Transformants of *Escherichia coli* BL21 carrying plasmid pGEX-5x-1 (containing GST) or derivatives containing different GST-GCN2 fusion proteins were cultured overnight at 37°C in Luria-Bertani medium containing ampicillin. Overnight cultures were diluted (1:100) into fresh Luria-Bertani-ampicillin medium and grown at 30°C. When the optical density at 600 nm reached ~0.8, isopropyl-β-D-thiogalactopyranoside (IPTG) was added to a final concentration of 0.1 mM and incubation was continued for 2.5 h to induce the expression of GST and GST fusion proteins. Cells were harvested, and GST and GST fusion proteins were purified as described in the *GST Gene Fusion System Manual* from Pharmacia (23a) with the following modification. After the glutathione-Sepharose 4B beads containing bound proteins were washed, the proteins were eluted with elution buffer (100 mM Tris-HCl [pH 8.0], 120 mM NaCl, 0.1% Triton X-100, 20 mM glutathione) and dialyzed against buffer A (20 mM Tris-HCl [pH 7.5], 100 mM NaCl, 0.2 mM EDTA, 1 mM dithiothreitol) containing 12.5% glycerol.

In vitro transcription and translation. In vitro transcription and translation with ^{35}S-labeled methionine were carried out by use of the TNT T7 Coupled Reticulocyte Lysate System (Promega) according to the vendor's instructions. In vitro-translated proteins were partially purified by ammonium sulfate precipitation as described previously (1). The protein precipitates were resuspended in 50 μl of buffer A containing 12.5% glycerol.

GST-binding assays. Immobilization of GST fusion proteins on glutathione-Sepharose 4B beads was carried out by incubating the purified fusion proteins at 1 μg/μl of beads (bed volume) in buffer A containing 0.1% Triton X-100 at room temperature for 30 min with rocking. The beads were washed and resuspended in the same buffer. Five microliters of in vitro-translated ^{35}S-labeled proteins prepared as described above or yeast cell extracts containing 50 μg of proteins prepared as described above for coimmunoprecipitation assays was added to beads (10-μl bed volume) containing 10 μg of bound GST fusion proteins, and the volume was increased to 200 μl with buffer A. The mixtures were incubated at 4°C for 2 h with rocking. The beads were collected by brief centrifugation in a microcentrifuge, washed three times with 500 μl of buffer A, resuspended in 40 μl of Laemmli sample buffer (17), and fractionated by SDS-PAGE. For detecting ^{35}S-labeled proteins, the gels were fixed with destaining buffer (25% methanol, 12% acetic acid), stained with Coomassie blue, treated with Amplify (Amersham), dried, and subjected to fluorography at −70°C. The results of Coomassie blue staining confirmed that similar amounts of each GST protein were bound to the beads in the different reaction mixtures. For detecting unlabeled proteins from cell extracts, fractionated proteins were transferred to nitrocellulose membranes and subjected to immunoblot analysis with anti-LexA antibodies (1:7,000 dilution), and the ECL system was used to visualize immune complexes.

RESULTS

Yeast two-hybrid analysis suggests that GCN2 dimerizes through the PK and C-term domains. GCN2 contains several domains flanking the PK domain that are required for its ability to phosphorylate eIF2α and derepress *GCN4* translation in amino acid-starved cells (31, 32) (Fig. 1A). We used the yeast two-hybrid assay to investigate whether the different domains in GCN2 can physically interact with one another. Two sets of plasmids carrying various segments of GCN2 either fused to bacterial LexA and expressed from the yeast constitutive *ADH1* promoter or fused to the B42 transcriptional activation domain and expressed from the galactose-inducible *GAL1* promoter were constructed. These plasmids were introduced in all pairwise combinations into yeast strain EGY48, containing a *LEU2* allele with LexA operators in place of the native transcriptional enhancer. Interaction between a pair of LexA and B42 fusions leads to activation of *LEU2* transcription and growth on medium lacking leucine. The results shown in Fig. 1B indicated that about two-thirds of the C-term kinase domain [′PK(720-999)] fused to LexA could interact with itself, with a slightly smaller kinase domain segment [′PK(750-999)], and with the C-term domain [C-term (1498-1659)], all fused to the B42 activation domain (Fig. 1B, row 4). Similar results were obtained with a LexA fusion containing ′PK(750-999), except that this smaller kinase domain segment did not interact with itself (Fig. 1B, row 5). A LexA fusion containing the C-term segment showed a strong interaction with itself and a moderate interaction with the larger of the two B42-PK fusions [′PK(720-999)] (Fig. 1B, row 8). The B42 fusions containing both ′PK segments and the C-term segment also interacted with full-length LexA-GCN2 (Fig. 1B, row 9). These results provided in vivo evidence for both homomeric and heteromeric interactions involving the PK and C-term domains of GCN2.

Given the self-interactions involving the ′PK and C-term segments, it was conceivable that the heteromeric interactions observed between the ′PK and C-term domains were indirect, involving three-component complexes where the ′PK and C-term domains interacted with the same full-length GCN2 molecules instead of directly interacting with one another. To eliminate this possibility, we deleted *GCN2* from the yeast strain used for two-hybrid analysis and reexamined selected two-hybrid constructs for interactions in the absence of native GCN2. We found that transformants of a *gcn2*Δ strain (HQY132) expressing the combinations of fusion proteins LexA-′PK(720-999) and B42-′PK(720-999), LexA-′PK(720-999) and B42–C-term, LexA–C-term and B42-′PK(720-999), or LexA–C-term and B42–C-term all showed two-hybrid interactions (galactose-dependent Leu$^+$ phenotypes) indistinguishable from those shown in Fig. 1B for these same constructs in the *GCN2* strain (data not shown).

To quantitate the two-hybrid interactions, we measured β-galactosidase expressed from a *lexAop-lacZ* reporter in selected transformants shown in Fig. 1B. As shown in Table 2, the β-galactosidase activity in the strain containing LexA–C-term and B42–C-term was ~100-fold higher than that in the strain containing LexA–C-term and the empty B42 vector (6,500 versus 60 U), verifying a strong self-interaction for the C-term domain. The other significant interaction observed was between the B42–C-term and LexA-′PK(720-999) fusion proteins, which showed 150 U of activity compared to 40 U for the LexA-′PK(720-999) and B42 fusion proteins (Table 2); however, we did not observe a significant self-interaction for the ′PK(720-999) segment with the *lacZ* reporter assay (Table 2). We interpret these findings to indicate that the self-interaction of ′PK(720-999) and the ′PK(720-999)–C-term heteromeric interaction are weaker than the C-term self-interaction and, consequently, are influenced by differences in fusion protein junctions or the promoter structures of the reporters. This interpretation is supported by the results of in vitro protein binding experiments described below.

Biochemical evidence for homomeric and heteromeric interactions involving the PK and C-term domains of GCN2. To obtain biochemical evidence for interactions involving the PK

A.

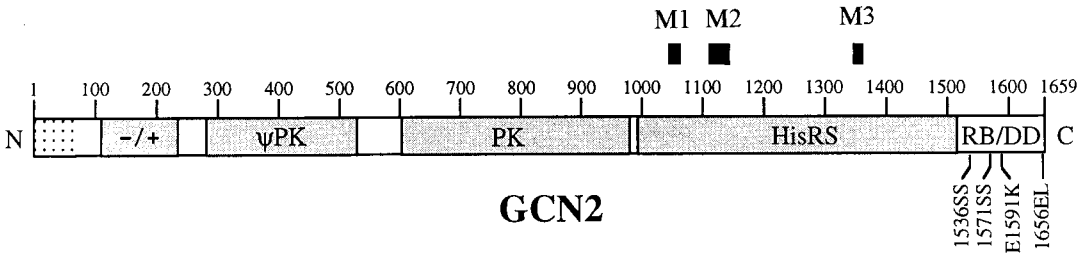

B.

Row	Column / LexA-fusions \ B42-fusions	A Protein expression	B B42 vector	C aa. 82-551 +/- and ψPK	D aa. 230-604 ψPK	E aa. 720-999 'PK	F aa. 750-999 'PK	G aa. 970-1497 HisRS	H aa. 1080-1497 HisRS	I aa. 1150-1497 HisRS	J aa. 1498-1659 C-term.
1	Protein expression		ND	+	+	+	+	+	+	+	+
2	bicoid	ND	−	−	−	−/+	−/+	−	−	−	−
3	aa. 230-604 ψPK	+	−	−	−	−	−	−	−	−	−
4	aa. 720-999 'PK	+	−	−	−	**+**	**+**	−	−	−	**+**
5	aa. 750-999 'PK	+	−	−	−	**+**	−/+	−	−	−	**+/−**
6	aa. 970-1497 HisRS	+	−	−	−	−/+	−	−	−	−	−/+
7	aa. 1080-1497 HisRS	+	−	−	−	−	−	−	−	−	−
8	aa. 1498-1659 C-term.	+	−	−	−	**+/−**	−	−	−	−	**+**
9	Full-length GCN2	+	−	−	−	**+**	**+**	−	−	−	**+**

FIG. 1. Yeast two-hybrid analysis of interactions between regulatory domains in GCN2. (A) Location of protein kinase and regulatory domains in GCN2. The rectangular box represents the GCN2 polypeptide chain from the amino (N) to carboxyl (C) terminus with the amino acid residues numbered from 1 to 1659. The N-terminal 69 amino acids (stippled region in the box) were appended to 1,590 residues published previously (31) based on recent findings indicating that the *GCN2* open reading frame begins at the 5′-most-in-frame ATG codon at position 1 (unpublished observations). As a result, all GCN2 amino acid positions in this report, including those in *GCN2* allele designations, are increased by 69 from the values indicated in previous publications. The different domains, including a highly charged region in the N terminus (−/+), a degenerate protein kinase domain (ψPK), the PK domain, a HisRS-related region, and a C-term region required for ribosome association and dimerization by GCN2 (RB/DD), are delineated in the rectangular box. The filled boxes above the GCN2 schematic indicate the positions of three sequence motifs (M1 to M3) conserved among class II aminoacyl-tRNA synthetases. (B) Yeast two-hybrid analysis of domain interactions in GCN2. Two sets of plasmids carrying the indicated segments of GCN2 fused to either bacterial LexA or the B42 transcriptional activation domain were introduced in all pairwise combinations (indicated in rows 2 to 9 and columns B to J) into yeast strain EGY48. Interaction between a pair of LexA and B42 fusion proteins leads to activation of *LEU2* transcription and growth on medium containing galactose as a carbon source and lacking leucine. The + symbol in column A and row 1 indicates that the fusion proteins were expressed, as determined by immunoblot analysis of whole-cell extracts with anti-LexA antibodies for LexA fusion proteins or anti-HA antibodies for B42 fusion proteins. The +, +/−, −/+, and − symbols in the other columns and rows designate strong, moderate, weak, and no growth, respectively, on medium lacking leucine, indicative of two-hybrid interactions. Boldface type was used to indicate growth responses that were significantly above background levels obtained with the negative controls in row 2 and column C. Segments of GCN2 contained in the LexA and B42 fusion constructs are indicated by amino acid (aa.) positions in full-length GCN2 and the GCN2 domains they encompass. Full-length GCN2 includes amino acids from 27 to 1659. ND, not determined. Additional LexA fusion proteins (not shown) containing GCN2 segments from residues 82 to 551, 574 to 998, and 1150 to 1497 were found to possess intrinsic activation function, conferring a Leu^+ phenotype to EGY48 when present in combination with the empty B42 vector, and were not analyzed further.

TABLE 2. Activation of the *lexAop-lacZ* reporter by interactions between LexA and B42 fusion proteins[a]

Plasmid	Fusion protein	U of β-galactosidase activity for:	
		LexA-′PK (720-999)	LexA–C-term (1498-1659)
pHQ435	B42-ψPK(230-604)	20 (−)	50 (−)
pHQ428	B42-′PK(720-999)	60 (+)	50 (+/−)
pHQ430	B42-HisRS(970-1497)	20 (−)	50 (−)
pHQ314	B42–C-term(1498-1659)	150 (+)	6,500 (+)
pJG4-5	B42	40 (−)	60 (−)

[a] Plasmids encoding the indicated LexA- and B42-GCN2 segments were co-transformed into strain EGY48 carrying the *lexAop-lacZ* reporter plasmid pSH18-34. β-Galactosidase activities in whole-cell extracts of these transformants were determined as described in Materials and Methods. The results shown are averages of activities from three or more individual transformants. The standard deviations for these averages were less than 30%. Symbols in parentheses indicate the strength of the two-hybrid interactions shown in Fig. 2 assayed with the *lexAop-LEU2* reporter.

and C-term segments, we carried out in vitro protein-binding assays with purified GST fusion proteins expressed in *E. coli* and some of the LexA fusion proteins used in two-hybrid assays described above. Equivalent amounts of GST fusion proteins containing the C-term segment (1498 to 1659) or the full-length PK domain (568 to 998) immobilized on glutathione-Sepharose beads were incubated with yeast extracts containing the LexA fusion proteins listed across the top of Fig. 2. The LexA fusion proteins that remained bound to the GST proteins after extensive washing of the beads were visualized by immunoblot analysis with antibodies against LexA. As expected, LexA alone did not interact detectably with any of the GST fusion proteins (Fig. 2, lanes 2 to 4), nor did any of the LexA-GCN2 segments interact with GST alone (Fig. 2, lanes 6, 10, 14, and 18). In contrast, significant fractions of LexA-′PK (720-999) bound to the GST-PK(568-998) and GST–C-term (1498-1659) fusion proteins (Fig. 2, lanes 11 and 12). A very small fraction of input LexA–C-term(1498-1659) was recovered with GST-PK(568-998), but a much larger proportion of this LexA fusion protein bound to GST–C-term(1498-1659) (Fig. 2, lanes 19 and 20). These findings are in accordance with the combined results of the two-hybrid analyses shown in Fig. 1B and Table 2 in demonstrating a strong self-interaction of the C-term segment and relatively weaker PK self-interaction and PK–C-term heteromeric interaction.

Although no significant interactions involving the ψPK and HisRS segments were detected with the two-hybrid assay (Fig. 1B), the LexA-ψPK and LexA-HisRS fusion proteins interacted in vitro with both GST-PK(568-998) and GST–C-term (1498-1659) segments but not with GST alone (Fig. 2, lanes 7, 8, 15, and 16). Because the GST-HisRS and GST-ψPK fusion proteins expressed in *E. coli* were very unstable, we could not confirm the interactions between these domains and the PK and C-term domains in reciprocal GST binding assays; however, additional evidence for these interactions is provided below.

Evidence that interactions between the PK and C-term segments of GCN2 occur in the absence of other yeast proteins. It was conceivable that the interactions that we detected for the C-term and PK domains of GCN2 with themselves and with one another were indirect and were mediated by some other yeast protein(s), such as GCN1 or GCN20 (20). To establish that these segments can interact with one another in the absence of all other yeast proteins, we carried out in vitro protein-binding assays with the GST-PK(568-998) and GST–C-term(1498-1659) fusion proteins and different GCN2 segments translated in rabbit reticulocyte lysates in the presence of [^{35}S] methionine. As expected, none of the labeled GCN2 segments interacted with GST alone (Fig. 3A to D), and in vitro-translated luciferase showed no detectable interaction with the GST-PK and GST–C-term fusion proteins (Fig. 3E). Quantitation of the binding data showed that small fractions of the input labeled PK(568-998) protein were precipitated with the GST–C-term (0.5%) and GST-PK (0.6%) fusion proteins; similarly, a small fraction of the labeled C-term(1498-1659) segment was recovered with the GST-PK fusion protein (1.9%) (Fig. 3F). Although the amounts of the bound fractions were small, they exceeded the background levels of binding to GST alone by more than 1 order of magnitude (Fig. 3F). A much

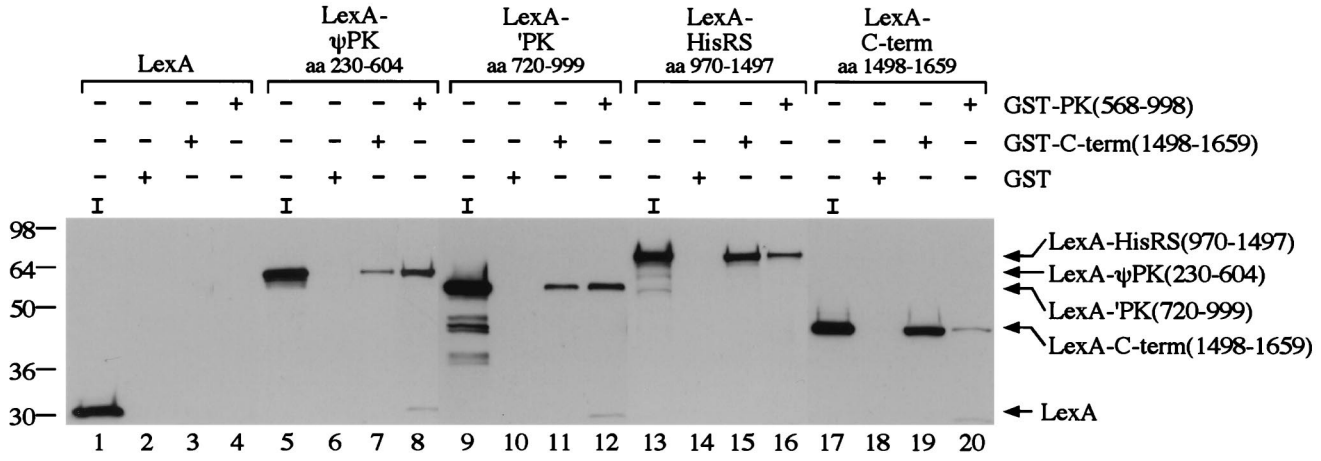

FIG. 2. In vitro binding of LexA fusion proteins containing different GCN2 segments, expressed in yeast, to GST fusion proteins containing the GCN2 PK and C-term domains. Aliquots of whole-cell extracts (50 μg of total protein) from transformants of yeast *gcn2*Δ strain HQY132 carrying plasmids containing the LexA fusion proteins indicated across the top were incubated with approximately equivalent amounts of GST, GST–C-term(1498-1659), or GST-PK(568-998) fusion proteins immobilized on glutathione-Sepharose beads. After extensive washing, LexA fusion proteins bound to the beads were resolved by SDS-PAGE and detected by immunoblot analysis with anti-LexA antibodies. Transformants of strain HQY132 contained the following plasmids: pEG202 (LexA), pHQ385 [LexA-ψPK(230-604)], pHQ433 [LexA-′PK(720-999)], pHQ426 [LexA-HisRS(970-1497)], and pHQ311 [LexA–C-term(1498-1659)]. Whole-cell extract (12.5 μg) (input, lanes I) or the bound fraction recovered from 25 μg of extract was loaded in each lane. aa, amino acids. Numbers at the left of gel are kilodaltons.

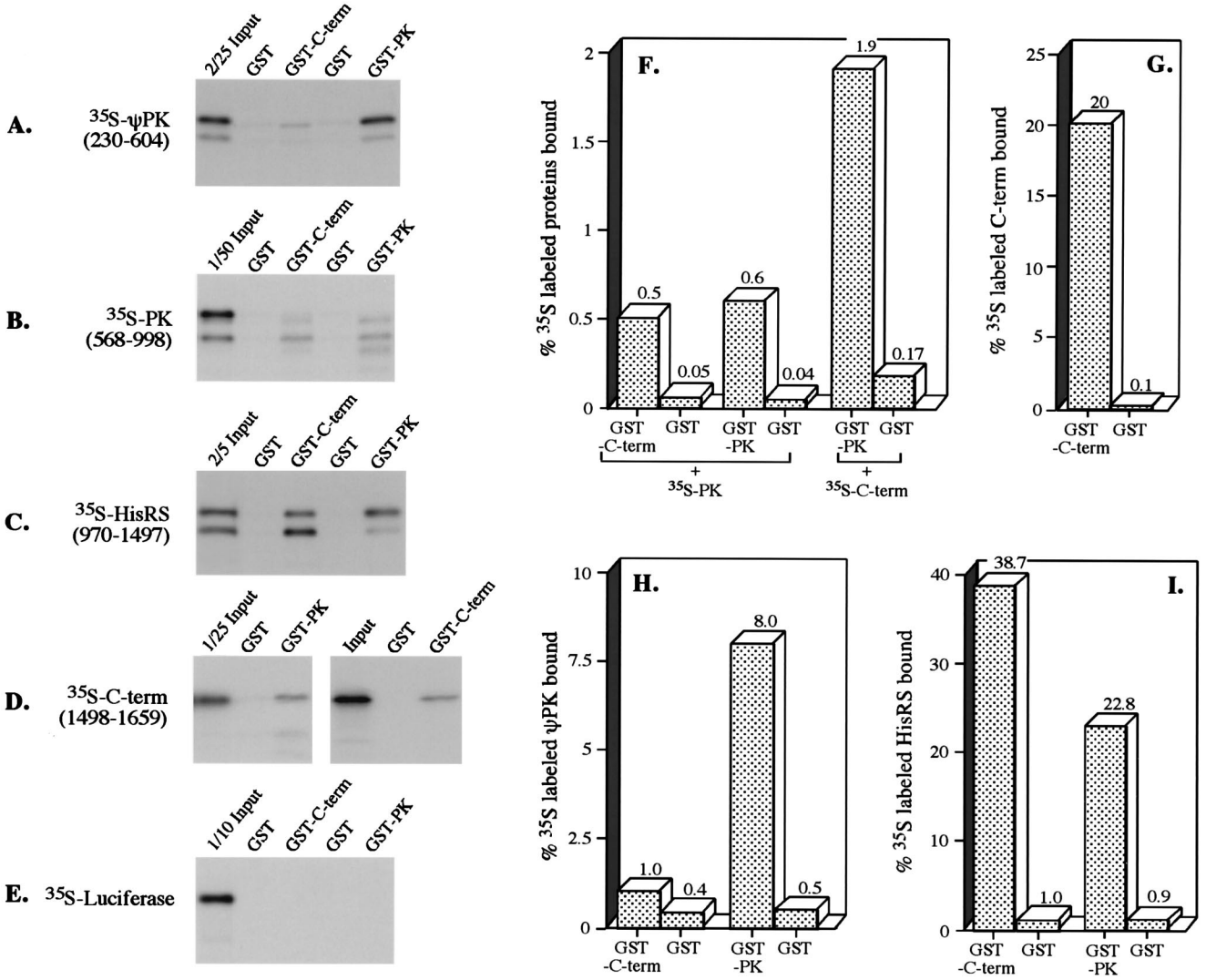

FIG. 3. In vitro binding of GCN2 segments translated in vitro to GST fusion proteins containing the GCN2 PK and C-term domains. (A to E) The GCN2 segments indicated to the left of panels A to D or the control protein luciferase (panel E) was translated in vitro with [^{35}S]methionine and incubated with GST, GST–C-term (1498-1659), or GST-PK(568-998) immobilized on glutathione-Sepharose beads. After a wash, the precipitated proteins were resolved by SDS-PAGE and visualized by fluorography. The leftmost lane in each panel contains the indicated fraction of the input radiolabeled protein used in the binding experiments. (F to I) Densities of bands in the autoradiograms in panels A to D were quantitated with a scanner (Silverscanner III) and NIH Image software (version 1.61). The data were plotted as the percentage of input radioactivity recovered in the fraction bound to the GST fusion protein.

larger fraction of the labeled C-term(1498-1659) segment was recovered with the GST–C-term fusion protein (20%) (Fig. 3D and G). The labeled ψPK segment interacted strongly with the GST-PK fusion protein (8% recovery; Fig. 3A and H), and the labeled HisRS(970-1497) fragment showed strong interactions with the GST-PK and GST–C-term fusion proteins (23 and 39% recoveries, respectively; Fig. 3C and I). The interaction of the labeled ψPK segment with the GST–C-term fusion protein was the weakest of all the interactions shown in Fig. 3, with the amount of bound fraction being only 2.5-fold larger than the background binding to GST alone (Fig. 3H). Together, these results are in agreement with the results of the GST pull-down experiments in Fig. 2 in showing relatively strong C-term self-interaction, strong PK-ψPK, PK-HisRS, and HisRS–C-term heteromeric interactions, and weaker but significant PK-PK and PK–C-term interactions.

Biochemical evidence that GCN2 dimerizes in vivo through self-interactions in the PK and C-term domains. To provide more direct evidence that GCN2 can dimerize in vivo, we examined whether native GCN2 could be immunoprecipitated from yeast whole-cell extracts with LexA fusion proteins containing different segments of GCN2. To this end, we fused the coding sequences for two tandem copies of the HA epitope to the genes encoding LexA and the LexA fusion proteins bearing GCN2 segments ψPK(230-604), ′PK(720-999), HisRS(970-1497), and C-term(1498-1659), used above for the two-hybrid analysis. A high-copy-number plasmid encoding wild-type GCN2 was introduced into strains expressing LexA-HA alone or LexA-HA fused to the different GCN2 segments. Extracts prepared from the resulting strains were immunoprecipitated with anti-HA antibodies, and the immune complexes were probed by immunoblot analysis with antibodies against LexA or GCN2. The results shown in Fig. 4 indicate that a substantial fraction of native GCN2 was coimmunoprecipitated with LexA-HA-′PK(720-999), whereas little or no GCN2 was recovered with LexA-HA-ψPK(230-604), LexA-HA-HisRS(970-1497), or

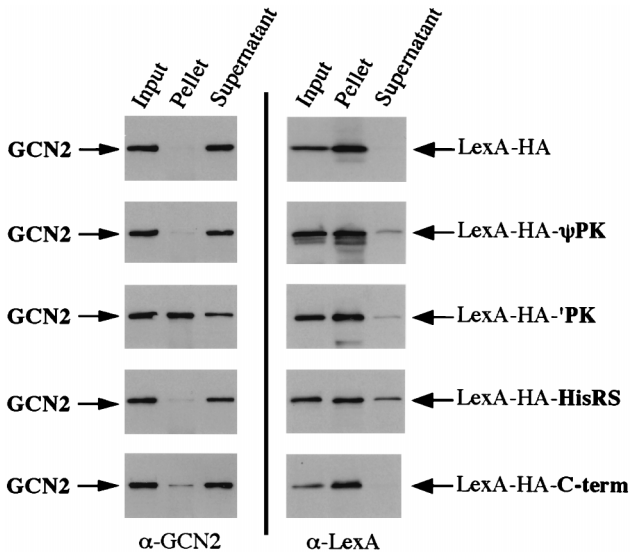

FIG. 4. Coimmunoprecipitation of native GCN2 with LexA-HA-GCN2 segments from yeast cell extracts. Transformants of *gcn2*Δ strain HQY132 bearing high-copy-number plasmid p630 encoding wild-type GCN2 and plasmids encoding the LexA fusion proteins indicated to the right of each panel were grown in liquid SC−Ura−His medium, and whole-cell extracts were prepared. Aliquots of extracts containing 50 μg of protein were incubated with protein A-agarose beads prebound with anti-HA antibody. Whole-cell extract (5 μg) (Input), immune complexes precipitated from 25 μg of extract (Pellet), and supernatant fractions corresponding to 5 μg of starting extract (Supernatant) were resolved by SDS-PAGE (8 to 16%) and transferred to nitrocellulose membranes. One portion of the blots was probed with anti-GCN2 antibodies (left panels), and the other portion was probed with anti-LexA antibodies (right panels). The following plasmids encoding LexA fusion proteins were used: p2247 (LexA-HA), pHQ385 [LexA-HA-ψPK(230-604)], pHQ587 [LexA-HA-′PK(720-999)], pHQ588 [LexA-HA-HisRS(970-1497)], and pHQ589 [LexA-HA–C-term(1498-1659)].

LexA-HA alone. A small fraction of GCN2 was coimmunoprecipitated with LexA-HA–C-term(1498-1659), and this amount was reproducibly larger than the background amount obtained with LexA-HA alone. These findings are consistent with the idea that GCN2 can dimerize through homomeric interactions involving the PK and C-term domains. The much greater recovery of GCN2 with ′PK(720-999) than with the C-term domain in these experiments is ostensibly at odds with the previous experiments indicating a stronger homomeric interaction of isolated C-term than of PK segments. Perhaps a weaker self-interaction of the LexA-HA-′PK protein than of the LexA-HA–C-term protein results in relatively lower amounts of free LexA-HA–C-term being available for dimerization with GCN2. Interdomain interactions in full-length GCN2 may increase the ability of the PK domain to dimerize with Lex-HA-′PK or decrease the ability of the C-term domain to interact with LexA-HA–C-term, relative to the self-interactions of the isolated segments in LexA fusions.

To provide additional in vivo evidence that the C-term domain alone can form a heterodimer with native GCN2, we examined whether overexpression of this segment would interfere with the function of GCN2 in phosphorylating eIF2. Strain H1613 contains the *GCN2*^{c}*-M788V,E1606G* allele, encoding an activated form of GCN2 that phosphorylates eIF2 at high levels under both starvation and nonstarvation conditions. This leads to a general inhibition of translation initiation and a reduction in the growth rate (25) that is completely dependent on the phosphorylation site at Ser-51 in eIF2α (6). We introduced into strain H1613 a high-copy-number plasmid encoding the C-term(1498-1659) segment expressed under the control of a strong galactose-regulated promoter (pHQ502) or just the empty vector pEMBLyex4 and compared the rates of colony formation of the resulting transformants. With galactose (but not glucose) as a carbon source, the transformants bearing pHQ502 formed substantially larger colonies than those containing the empty vector (data not shown). A similar result was obtained with overexpression of the C-term lobe of the GCN2 PK domain (5a). These results can be explained by proposing that overexpression of the C-term or ′PK segments disrupts GCN2^c-GCN2^c homodimers and replaces them with less active GCN2^c–C-term(1498-1659) or GCN2^c-′PK heterodimers.

We showed above that PK segments were capable of heteromeric interactions with isolated ψPK, HisRS, and C-term segments in addition to PK self-interactions (Fig. 2 and 3). Accordingly, we wished to determine whether the interaction between full-length GCN2 and LexA-HA-′PK(720-999) shown in Fig. 4 is mediated by PK self-interactions or by heteromeric interactions between LexA-HA-′PK(720-999) and the ψPK, HisRS, or C-term domain in GCN2. If the former is true, the interaction should be abolished by deletion of the PK domain but relatively unaffected by deletion of the ψPK, HisRS, or C-term domain from GCN2. In agreement with this prediction, the results shown in Fig. 5 indicate that deletion of the entire PK domain from GCN2 abolished its coimmunoprecipitation with LexA-HA-′PK(720-999). In contrast, deleting most of the C-term domain had no effect, and removing nearly all of the ψPK domain or a segment containing most of the HisRS and half of the C-term domains reduced the coimmunoprecipitation of GCN2 with LexA-HA-′PK(720-999) by only ≈60 or ≈25%, respectively. Thus, dimerization between isolated PK and full-length GCN2 is dominated by PK self-interactions. It is noteworthy that the LexA-HA-ψPK and LexA-HA-HisRS fusion proteins did not detectably interact with full-length GCN2 in the experiments shown in Fig. 4, despite their strong interactions with isolated PK and C-term segments in GST fusions (Fig. 2 and 3). This finding can be explained by proposing that intramolecular interactions with the endogenous ψPK and HisRS segments prevent the PK and C-term domains in native GCN2 from interacting with exogenous ψPK and HisRS segments fused to LexA.

To demonstrate that full-length GCN2 molecules can dimerize in vivo, we carried out immunoprecipitation experiments with strains coexpressing wild-type GCN2 and full-length LexA-HA-GCN2. As shown in Fig. 6, ≈20% of wild-type GCN2 in cell extracts was coimmunoprecipitated with LexA-HA-GCN2 by use of anti-HA antibodies (panel A, lanes 1, 6, and 11, and panel C, wt), whereas no detectable GCN2 was coimmunoprecipitated with LexA-HA (panel B, lanes 1, 6, and 11). A comparison of lanes 1 and 11 of Fig. 6A suggests that LexA-GCN2 forms homodimers with itself more efficiently than it forms heterodimers with native GCN2. This preference may reflect the fact that LexA itself has a dimerization function (27). The formation of homodimers may also be favored if dimerization is coincident with translation. In view of these considerations, the fact that ≈20% of GCN2 forms heterodimers with LexA-HA-GCN2 probably indicates that a large fraction of full-length GCN2 is dimerized in cell extracts.

We next examined whether the C-term or PK domain is required for dimerization by full-length GCN2 molecules. We found that deletion of most of the ψPK domain did not reduce the coimmunoprecipitation of GCN2 with LexA-HA-GCN2 by use of anti-HA antibodies (Fig. 6A, lanes 2, 7, and 12, and 6C, Δ324-538), whereas deletion of the entire PK domain and the N-terminal end of the HisRS domain reduced coimmunoprecipitation by about one third relative to that of wild-type GCN2. Similarly, a deletion that removed the C-term two

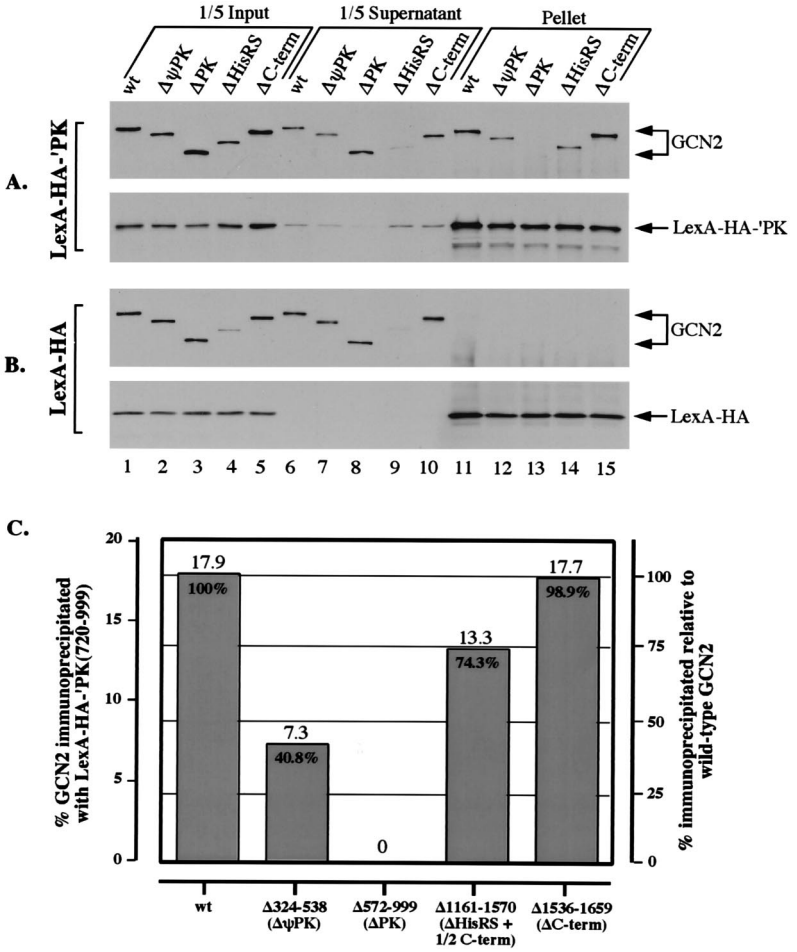

FIG. 5. Coimmunoprecipitation of GCN2 with LexA-HA-PK requires the PK domain in GCN2. (A) Whole-cell extracts were prepared from transformants of *gcn2*Δ strain HQY132 bearing high-copy-number plasmid pHQ587 containing LexA-HA-′PK(720-999) and plasmids containing wild-type GCN2 (p630) or one of the following deletion mutants: gcn2-Δ324-538(ΔψPK) (p2327), gcn2-Δ572-999(ΔPK) (pB82), gcn2-Δ1161-1570(ΔHisRS+1/2C-term) (p2463), or gcn2-Δ1536-1659(ΔC-term) (p2461). Aliquots of extracts containing 50 μg of protein were immunoprecipitated with anti-HA antibodies, and the immune complexes were resolved by SDS-PAGE and subjected to immunoblot analysis with anti-GCN2 antibodies (upper panel) or anti-LexA antibodies (lower panel), all as described in the legend to Fig. 4. Lanes 1 to 5 contain 5 μg of extract used for the immunoprecipitations, lanes 6 to 10 contain amounts of supernatants corresponding to 5 μg of starting extract from the immunoprecipitations, and lanes 11 to 15 contain amounts of pellets corresponding to 25 μg of starting extract from the immunoprecipitations. (B) Whole-cell extracts prepared from transformants of HQY132 harboring plasmid p2247 containing LexA-HA and either p630, p2327, pB82, p2463, or p2461 were immunoprecipitated with anti-HA antibodies, and the immune complexes were analyzed by immunoblot analysis with anti-GCN2 antibodies (upper panel) or anti-LexA antibodies (lower panel), with the same proportions of samples loaded as in panel A. (C) Densities of the bands in panel A for the input and pellet fractions were calculated with a scanner (Silverscanner III) and NIH Image software (version 1.61). The percentage of the input amount that was coimmunoprecipitated with LexA-HA-PK was calculated from two independent experiments, and the average was plotted for each GCN2 protein (scale on the left; averages shown above the bars). The percentage of the mutant protein that was coimmunoprecipitated with LexA-HA-GCN2 relative to wild-type GCN2 was also plotted (scale on the right; values shown inside the bars). wt, wild type.

thirds of the HisRS domain and the N-terminal one half of the C-term domain reduced coimmunoprecipitation by about one fourth. In contrast to these modest reductions, deletion of most of the C-term domain reduced the coimmunoprecipitation of GCN2 with LexA-HA-GCN2 to less than 10% the wild-type GCN2 level (Fig. 6A, lanes 4, 9, and 14, and 6C, Δ1536-1659). These results suggest that the C-term segment is the most important portion of GCN2 for dimerization by full-length molecules. This finding is in accordance with the two-hybrid and GST pull-down experiments indicating that the C-term segment has the strongest self-interaction among the isolated domains of GCN2.

Mapping the residues in the C-term domain required for self-interaction and interaction with the PK domain. We used the two-hybrid assay in an effort to identify specific segments of the C-term region of GCN2 that mediate its strong self-interaction. We began by introducing into both the LexA–C-term and the B42–C-term fusion proteins point mutations shown previously to alter the regulatory function of native GCN2. These included two different two-codon insertions at positions 1571 and 1656 that inactivate *GCN2* function (*gcn2-1571SS* and *gcn2-1656EL*) (31) and a substitution at Glu-1591 that leads to constitutive activation of *GCN2* function in vivo (25). Neither these point mutations nor a two-codon insertion at position 1536 that does not affect *GCN2* function (31) detectably altered the C-term self-interaction, as judged by the Leu phenotype of the yeast transformants (Fig. 7, no. 2 to 5, "Self"-LexA fusion). We next analyzed the effects of nested N-terminal and C-term deletions in the LexA- and B42–C-term constructs on self-interaction in the two-hybrid assay. The results obtained with the N-terminal deletions indicated that self-association of the C-term segment required residues between positions 1498 and 1535 (Fig. 7, no. 6 to 9). Truncation from the C terminus to position 1635 had no effect on the interac-

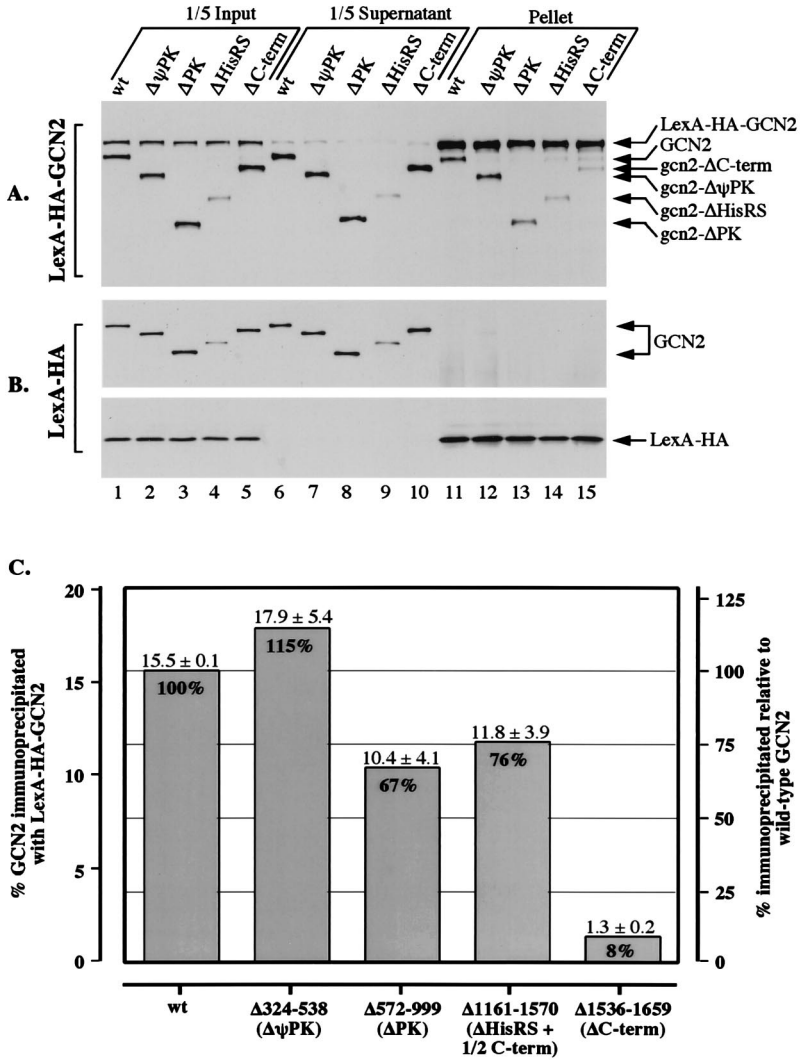

FIG. 6. Coimmunoprecipitation of mutant and wild-type GCN2 proteins with full-length LexA-HA-GCN2. (A) Whole-cell extracts were prepared from transformants of *gcn2*Δ strain HQY132 bearing high-copy-number plasmid pHQ400 containing LexA-HA-GCN2 and plasmids containing wild-type GCN2 (p630) or one of the following deletion mutants: gcn2-Δ324-538(ΔψPK) (p2327), gcn2-Δ572-999(ΔPK) (pB82), gcn2-Δ1161-1570(ΔHisRS+1/2C-term) (p2463), or gcn2-Δ1536-1659(ΔC-term) (p2461). Aliquots of extracts containing 50 μg of protein were immunoprecipitated with anti-HA antibodies, and the immune complexes were resolved by SDS-PAGE and subjected to immunoblot analysis with anti-GCN2 antibodies, all as described in the legend to Fig. 4. Lanes 1 to 5 contain 5 μg of extract used for the immunoprecipitations, lanes 6 to 10 contain amounts of supernatants corresponding to 5 μg of starting extract from the immunoprecipitations, and lanes 11 to 15 contain amounts of pellets corresponding to 25 μg of starting extract from the immunoprecipitations. (B) Whole-cell extracts prepared from transformants of HQY132 harboring plasmid p2247 containing LexA-HA and either p630, p2327, pB82, p2463, or p2461 were immunoprecipitated with anti-HA antibodies, and the immune complexes were analyzed by immunoblot analysis with anti-GCN2 antibodies (upper panel) or anti-LexA antibodies (lower panel), with the same proportions of samples loaded as in panel A. (C) Densities of the bands in panel A for the input and pellet fractions were calculated with a scanner (Silverscanner III) and NIH Image software (version 1.61). The percentage of the input amount that was coimmunoprecipitated with LexA-HA-GCN2 was calculated from three or more independent experiments, and the average was plotted for each GCN2 protein (scale on the left; averages ± standard deviations shown above the bars). The percentage of the mutant protein that was coimmunoprecipitated with LexA-HA-GCN2 relative to wild-type GCN2 was also plotted (scale on the right; values shown inside the bars). wt, wild type.

tion (Fig. 7, no. 10), whereas the protein truncated at position 1610 had intrinsic activation function and could not be analyzed (no. 11). The protein with the Δ1585-1659 truncation failed to interact (Fig. 7, no. 12); however, this protein was expressed at relatively low levels (Fig. 8, lane 6), making it unclear whether an important interaction domain is located C terminal to position 1585.

To localize the interaction determinants in the C-term segment more precisely, we analyzed the internal deletions shown in Fig. 7 (no. 6 and 13 to 19, "Self"-LexA fusion). The results of this analysis confirmed the presence of an important region between residues 1498 and 1535, as internal deletions of residues 1498 to 1517 or 1518 to 1537 reduced the two-hybrid interaction (Fig. 7, no. 6 and 13). The fact that deletion of all of the residues between positions 1498 and 1535 abolished the interaction (Fig. 7, no. 7) suggests that this domain is multipartite and that a weak interaction can be achieved with either its N-terminal or its C-term subdomain. The fact that deleting residues 1536 to 1570 weakened the interaction (Fig. 7, no. 19) whereas deleting residues 1558 to 1577 did not (no. 15) suggests that the C-term boundary of the N-terminal interaction domain is located between residues 1537 and 1558. Examination of constructs 15 to 18 in Fig. 7 suggests that a second critical interaction domain is located between residues 1578 and 1597, and the results obtained with constructs 10, 17, and 18 suggest that the region located C terminal to position 1597

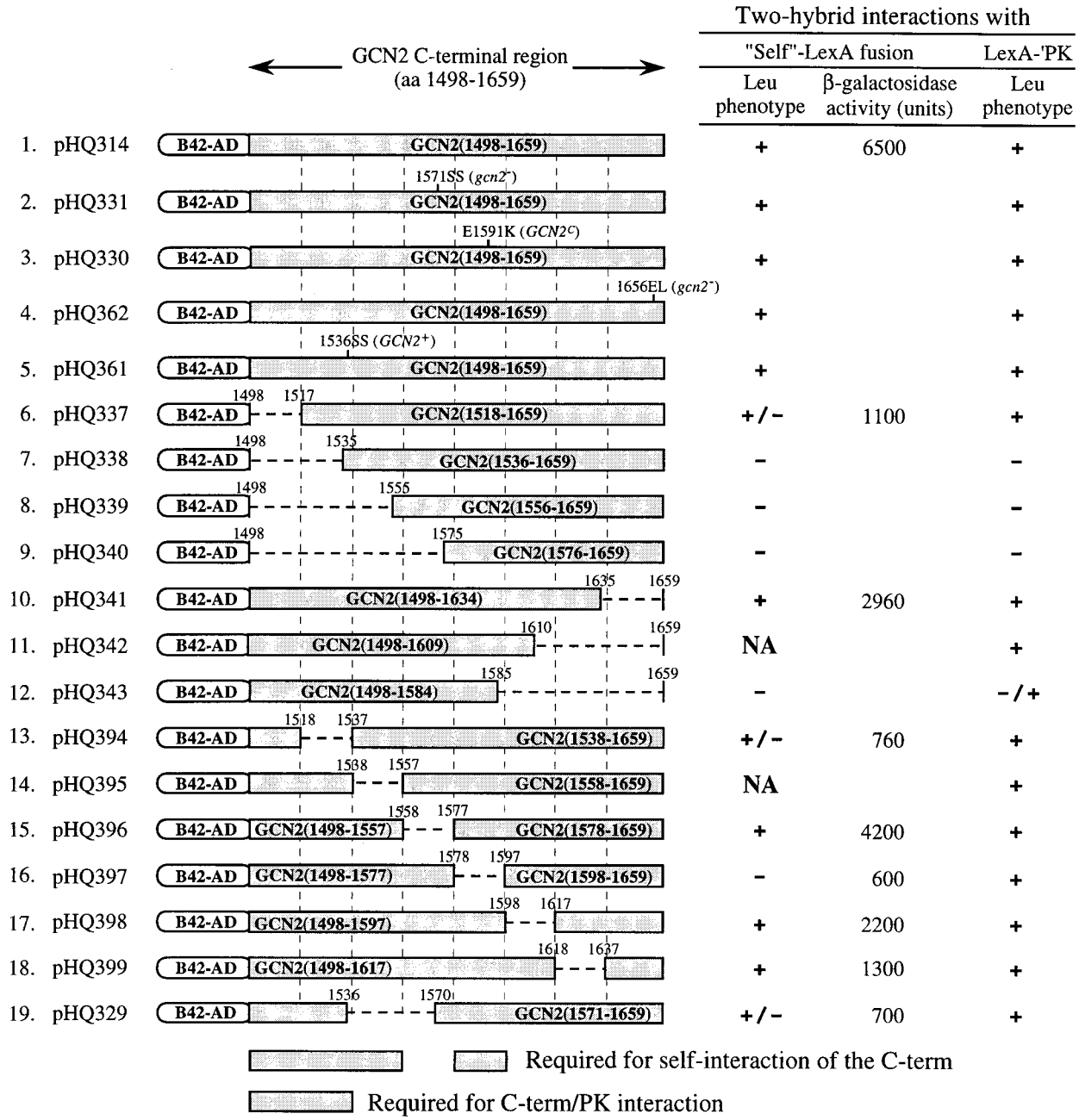

FIG. 7. Deletion mapping of interaction determinants in the C-term region that mediate self-interaction and interaction with the PK domain in the two-hybrid assay. The GCN2 C-term region (residues 1498 to 1659) and deletion derivatives (depicted by gray rectangular boxes) were fused to the B42 activation domain (open box) in plasmid pJG4-5, producing the constructs listed on the left, and to LexA in plasmid pEG202 (not shown). Broken lines represent amino acids (aa) deleted from the C-term segments, as indicated by the numbers above the lines indicating the first and last amino acids deleted in each construct. For determination of two-hybrid interactions between the LexA and B42 fusion proteins containing identical C-term segments (interactions with "Self"-LexA fusion), strain EGY48 was cotransformed with the appropriate LexA and B42 fusion plasmids. For determination of two-hybrid interactions between the LexA-′PK(720-999) and B42–C-term fusion proteins, EGY48 was cotransformed with plasmid pHQ433 containing LexA-′PK(720-999) and the constructs listed on the left containing B42–C-term fusion proteins. The resulting transformants were tested for growth on SGal/Raf+Ura medium, indicative of a two-hybrid interaction that activates the expression of the *lexAop-LEU2* reporter (Leu phenotype). +, +/−, −/+, and −, strong, moderate, weak, and no growth, respectively; NA, not applicable, because the LexA fusion proteins conferred a Leu^+ phenotype in the absence of a B42 fusion protein. Selected transformants containing LexA and B42 fusion proteins bearing the same C-term segments (self-interactions) were also analyzed for β-galactosidase activities in the cell extracts, indicating a two-hybrid interaction that activates the expression of the *lexAop-lacZ* reporter. The activities shown are averages calculated from results obtained with three or more independent transformants and expressed as nanomoles of *o*-nitrophenyl-β-D-galactopyranoside hydrolyzed per minute per milligram of protein. The standard deviations were less than 30% of the averages.

is dispensable for self-interaction, at least in the presence of the more N-terminally located interaction determinants. We also analyzed the expression of the *lacZ* reporter in the transformants bearing internal deletions in the C-term fusion proteins, and the results of these β-galactosidase assays were generally in agreement with the corresponding Leu^+ phenotypes (Fig. 7, "Self"-LexA fusion). Judging by the β-galactosidase activities, it appears that deletions of residues in the intervals

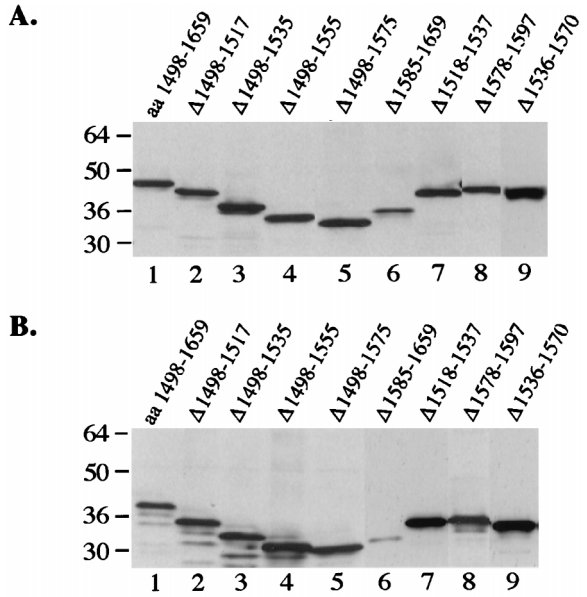

FIG. 8. Expression of selected LexA and B42 fusion proteins bearing different portions of the GCN2 C-term domain used for two-hybrid analysis. Transformants bearing plasmids containing LexA or B42 fused to C-term(1498-1659) or their derivatives with the deletions indicated above the panels were grown to the log phase in liquid synthetic complete medium containing galactose and raffinose as carbon sources and lacking histidine and tryptophan to select for the plasmids. Whole-cell extracts were prepared, and aliquots containing 25 μg of protein were resolved by SDS-PAGE and subjected to immunoblot analysis with anti-LexA antibodies to detect LexA fusion proteins (A) and anti-HA antibodies to detect B42 fusion proteins (B). Immune complexes were visualized by ECL. Numbers at left of panels are kilodaltons.

from 1518 to 1537 and 1578 to 1597 are equally deleterious to the self-interaction of the C-term domain.

We wished to determine whether the residues in the C-term segment that mediate self-interaction are also involved in the interaction between the C-term and PK domains. To answer this question, we tested the point mutations and deletions in the C-term–B42 fusion proteins just described for interactions with the LexA-′PK(720-999) fusion protein. As shown in Fig. 7 (LexA-′PK), the multipartite domain located between residues 1498 and 1558 is required for the interaction between the PK and C-term segments; however, it appears that a strong interaction can be achieved with either the N-terminal or the C-term segments from this region (Fig. 7, compare no. 7 with no. 6, 13, and 14). The second domain required for C-term self-interaction, located between residues 1578 and 1597, is not required for the interaction with the ′PK domain (Fig. 7, no. 16). Thus, interaction between the ′PK and C-term domains appears to require a subset of the determinants required for C-term self-interaction in the two-hybrid assay (Fig. 7, summary at bottom).

We also attempted to identify discrete segments in the PK domain required for self-interaction and for its association with the C-term segment by making 30-amino-acid internal deletions across the ′PK(720-999) segment in the LexA and B42 fusion proteins containing this segment. As already described in Fig. 1B, the construct which lacks the N-terminal 30 residues [′PK(750-999)] interacted with both the ′PK and the C-term segments. In contrast, all of the other internal deletions abolished the ability of the ′PK(720-999) segment to interact with itself and with the C-term segment, despite the fact that the fusion proteins with internal deletions were well expressed (data not shown). We presume that both interactions depend on the intact tertiary structure of the ′PK(750-999) domain, which was probably disrupted by each of the internal deletions that we examined.

The entire C-term segment of GCN2 is required for its regulatory function in vivo. If the two regions in the C-term domain required for self-interaction of this domain in the two-hybrid assay are also important for the dimerization of native GCN2 and if dimerization is required for GCN2 activation or catalytic function, then deletions of these regions in full-length *GCN2* should reduce its function in vivo. To test this prediction, we introduced into an otherwise wild-type *GCN2* allele on a low-copy-number plasmid the eight consecutive 20-codon deletions spanning residues 1498 to 1659 that were analyzed in Fig. 7 (constructs 6, 10, and 13 to 18). The resulting *gcn2* alleles were tested for complementation of the 3-aminotriazole (3-AT)-sensitive phenotype of the *gcn2*Δ strain H1472. 3-AT inhibits histidine biosynthesis, and *gcn2*Δ mutants are 3-AT sensitive because they fail to induce the expression of *GCN4* and the histidine biosynthetic genes under GCN4 control. With the exception of *gcn2*Δ*-1498-1517*, which was indistinguishable from wild-type *GCN2*, all of the remaining 20-codon deletion alleles appeared to be completely nonfunctional. Of these, only the deletions from residues 1518 to 1537 and 1578 to 1597 led to significant reductions in protein expression which might have accounted for their 3-AT-sensitive phenotypes (Table 3). To eliminate this possibility, we inserted these alleles into a high-copy-number plasmid from which wild-type GCN2 is overexpressed 20- to 50-fold (32) and retested their phenotypes in the *gcn2*Δ strain. Both the *gcn2*-Δ*1518-1537* and *gcn2*-Δ*1578-1597* alleles retained their 3-AT-sensitive phenotypes when present on multicopy plasmids, confirming that the encoded proteins are nonfunctional.

DISCUSSION

Evidence for dimerization of GCN2 mediated by self-interactions in the C-term and PK domains. Using the yeast two-hybrid assay and in vitro binding studies with recombinant proteins, we found that the isolated PK and C-term domains of GCN2 can interact with themselves and that the self-interaction of the isolated C-term domain appears to be stronger than the PK-PK interaction. Using the two-hybrid assay and coimmunoprecipitation analysis, we showed that LexA fusion proteins containing the isolated PK and C-term domains can also

TABLE 3. Phenotypes of plasmid-borne *gcn2* alleles with internal deletions in the C-term region[a]

Plasmid	*gcn2* allele	Growth on 3-AT	Relative GCN2 protein level
p722	*GCN2*$^+$	+	1
pHQ406	*gcn2-Δ1498-1517*	+	1.4
pHQ402	*gcn2-Δ1518-1537*	−	0.2
pHQ407	*gcn2-Δ1538-1557*	−	2
pHQ408	*gcn2-Δ1558-1577*	−	2
pHQ409	*gcn2-Δ1578-1597*	−	0.4
pHQ403	*gcn2-Δ1598-1617*	−	0.8
pHQ405	*gcn2-Δ1618-1637*	−	1.4
pHQ404	*gcn2-Δ1638-1659*	−	1.8
Vector	None	−	None

[a] Plasmid-borne wild-type *GCN2* and *gcn2* alleles were introduced into *gcn2*Δ strain H1472, and the resulting transformants were tested for 3-AT sensitivity on synthetic minimal medium containing 10 mM 3-AT. +, growth indistinguishable from that given by wild-type *GCN2*; −, no growth. The relative level of GCN2 protein expressed from each allele was determined by SDS-PAGE and immunoblot analysis of whole-cell extracts with antibodies against GCN2.

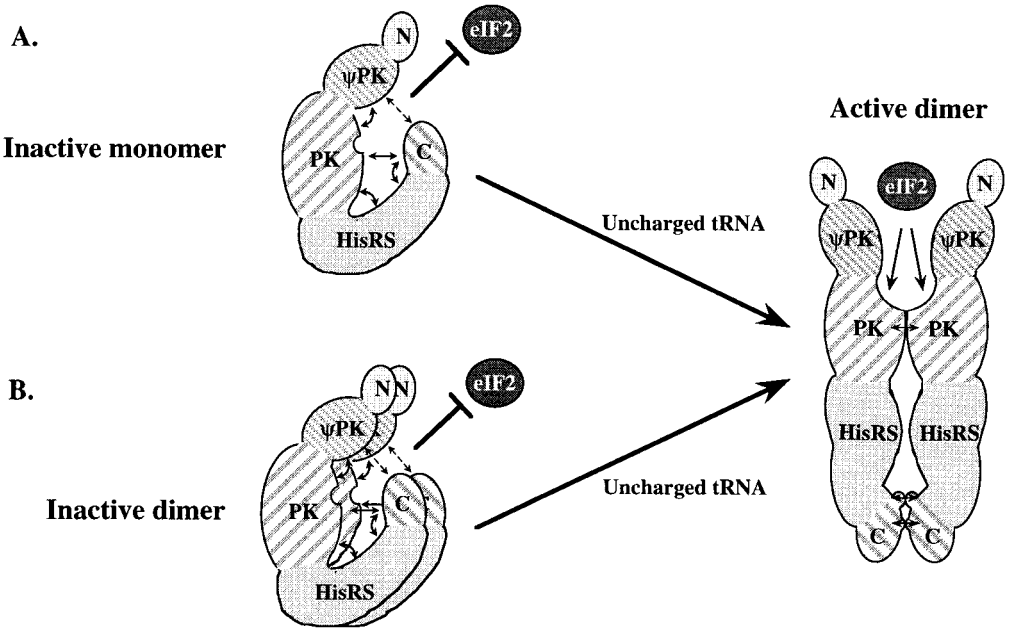

FIG. 9. Hypothetical model for the role of domain interactions and dimerization in the activation of GCN2 by uncharged tRNA. (A) Independent interactions between the PK domain and the C-term, HisRS, and ψPK regions contribute to the inactivity of the PK domain under nonstarvation conditions when uncharged tRNA is scarce. The strong interdomain interactions between the PK domain and the HisRS or ψPK region inhibit the dimerization function of PK, such that the inactive form of GCN2 is monomeric. The C-term domain functions as an autoinhibitory segment that blocks autophosphorylation by GCN2 and prevents the binding of substrates to the active site. Binding of uncharged tRNA to the HisRS region triggers a conformational change that replaces the inhibitory interdomain interactions with self-interactions for the PK and C-term segments, stabilizing the GCN2 dimer and dissociating the autoinhibitory C-term segment from the PK domain. *trans*-Autophosphorylation of GCN2 ensues in the dimer, altering the structure of the PK domain to permit binding and phosphorylation of the substrate eIF2. (B) Both the inactive and active forms of GCN2 are dimers. Interdomain interactions between the PK domain and the C-term, HisRS, and ψPK regions are responsible for inhibiting the PK domain when uncharged tRNA is scarce. Binding of uncharged tRNA to the HisRS region triggers a conformational change that dissociates the autoinhibitory C-term segment from the PK domain to permit autophosphorylation and binding of eIF2 to the active site.

form relatively stable complexes with full-length GCN2 in vivo. Deletion of the PK domain in GCN2 abolished its coimmunoprecipitation with LexA-′PK(720-999), confirming that complex formation between the isolated PK domain and full-length GCN2 was dependent on the PK self-interaction. We also showed by coimmunoprecipitation experiments that a substantial fraction of wild-type GCN2 could form a stable complex in vivo with a full-length LexA-HA-GCN2 fusion protein, providing direct evidence for dimerization by full-length GCN2 molecules. This interaction was abolished by deletion of the C-term domain, indicating that the C-term segment is critical for dimerization by full-length GCN2, whereas deletion of the PK domain led to only a modest reduction in complex formation. This last finding is in accordance with the fact that the self-interaction of isolated PK segments was weaker than that of isolated C-term segments.

Because the C-term domain appeared to be the most important for dimerization by full-length GCN2 proteins, we carried out a deletion analysis of this region in an effort to localize the amino acids that mediate its self-interaction in the two-hybrid assay. These experiments suggested the existence of multiple dimerization determinants mapping within the 100-residue C-term segment. Deletion of residues 1498 to 1535 or 1578 to 1597 was sufficient to abolish self-interaction of the C-term segment in the two-hybrid assay (Fig. 7). However, whereas deletion of the entire C-term segment from GCN2 abolished its coimmunoprecipitation with LexA-HA-GCN2, a deletion that removed only the dimerization determinant from residues 1498 to 1557 led to only a small reduction in complex formation by full-length GCN2 proteins (Fig. 6, ΔHisRS +1/2 C-term). The same result was obtained recently for the Δ1578-1597 mutation in GCN2, which removes the second C-term dimerization determinant (23b). We conclude that deletion of both dimerization determinants in the C-term domain is required to abolish dimerization by full-length GCN2 with LexA-HA-GCN2 under the conditions of our coimmunoprecipitation experiments. Perhaps removing only one of these determinants is sufficient to abolish self-interaction of the C-term domain in two-hybrid assays but not to eliminate dimerization by full-length GCN2 because, with the latter, self-interactions in the PK domain can compensate for a reduction in C-term domain self-interactions.

Although deletion of the entire C-term domain from full-length GCN2 abolished its dimerization with full-length LexA-HA-GCN2 (Fig. 6), the LexA fusion protein containing only ′PK(720-999) was coimmunoprecipitated with full-length GCN2 in the absence of any C-term self-interactions (Fig. 4). This apparent discrepancy cannot be explained by different protein concentrations in the two cases, because the LexA-HA-′PK(720-999) and LexA-HA-GCN2 fusion proteins and the full-length GCN2 and gcn2-Δ1536-1659(ΔC-term) proteins were expressed at similar levels (Fig. 6 and data not shown). Accordingly, it may indicate that the dimerization function of the PK domain is partially masked by other domains in GCN2, so that dimerization by full-length GCN2 molecules is critically dependent on the self-interactions of the C-term segments. In the absence of the putative interference of an adjacent domain(s), the isolated PK domain in LexA-HA-′PK(720-999) could interact more efficiently with the PK domain in full-length GCN2. Given that the PK domain showed strong interactions with both the ψPK and the HisRS domains (Fig. 2 and 3), one or both of these adjacent regions may interfere with the

dimerization function of the PK domain in full-length GCN2 (Fig. 9A).

Evidence that dimerization is important for *GCN2* function in vivo comes from the observation that the growth-inhibitory effects of a *GCN2*^{c} allele were reduced by coexpression of wild-type GCN2 (7). In addition, we found that overexpression of just the C-term segment of GCN2 interfered with the function of GCN2^c proteins in vivo. This dominant-negative phenotype is consistent with the formation of heterodimers with reduced kinase activity. In addition, we were able to isolate a substantial fraction of GCN2 in a complex with LexA-HA-GCN2 from whole-cell extracts, suggesting that much of GCN2 is dimerized in these extracts. Deletion of the entire C-term domain abolished coimmunoprecipitation of full-length GCN2 with LexA-HA-GCN2 (Fig. 6) and likewise destroyed *GCN2* function. While this finding is consistent with the idea that dimerization is required for GCN2 activity in vivo, deletion of the C-term domain also eliminates ribosome binding by GCN2 (24) and removes residues with important regulatory functions identified by *GCN2*^{c} mutations (25, 32). It is not known which of these functions is more critically required for GCN2 activity in vivo. As mentioned above, deletion of residues 1578 to 1597 in the C-term domain abolished C-term self-interaction in the two-hybrid assay and impaired *GCN2* function in vivo but did not eliminate coimmunoprecipitation of GCN2 with LexA-HA-GCN2 (unpublished observations). Thus, it may have destroyed *GCN2* function because it impaired ribosome binding or a regulatory interaction between the C-term and PK domains without affecting GCN2 dimerization. In fact, we recently found that the Δ1578-1597 mutation does weaken ribosome binding by GCN2 in cell extracts (8a). Alternatively, given the redundancy of dimerization determinants in the C-term and PK domains, this small deletion may substantially reduce dimerization only when GCN2 is expressed at wild-type levels. Addressing this last possibility will require a more sensitive assay for dimerization by full-length GCN2 than that used here, which involved coimmunoprecipitation of overexpressed GCN2 and LexA-HA-GCN2 proteins.

Another important issue is whether dimerization and ribosome binding are functionally related. Recently, we found that deletion of C-term residues 1558 to 1577, which are dispensable for the two-hybrid self-interaction of the C-term domain (Fig. 7), leads to a large reduction in ribosome binding by full-length GCN2 (8a). This finding, plus the incongruent effects of the Δ1578-1597 mutation on ribosome binding and dimerization cited above, suggests that dimerization is not dependent on ribosome binding and that the two functions have overlapping but nonidentical requirements for C-term residues. It remains to be determined whether ribosome binding is dependent on dimerization.

Dimerization plays an important role in the activation of cell surface receptor kinases by facilitating *trans*-autophosphorylation by the subunits of the dimer (13). A similar role for dimerization in stimulating autophosphorylation has been suggested for GCN2, with the added notion that the binding of tRNA to the HisRS domain would stabilize GCN2 dimers (7). This last suggestion was motivated partly by the fact that authentic histidyl-tRNA synthetase functions as a dimer (5). We did not detect self-interaction of the HisRS domain in the two-hybrid assay (Fig. 1B), nor did we observe dimerization of LexA-HA-HisRS with GCN2 in coimmunoprecipitation assays (Fig. 4), even when the extracts were prepared from histidine-starved cells (unpublished observations). In addition, the yield of GCN2–LexA-HA-GCN2 complexes detected by coimmunoprecipitation was not increased when the cells were grown under histidine starvation conditions (data not shown). These findings could be taken to indicate that dimerization is a constitutive function of GCN2 and is not dependent on elevated levels of uncharged tRNA in amino acid-starved cells (Fig. 9B). It is possible, however, that dimerization occurs in vitro following cell lysis due to high levels of deacylated tRNAs formed in the extracts, whether or not the cells are starved for amino acids prior to lysis. In accordance with this suggestion, it was shown that GCN2 kinase activity in cell extracts is dependent on the HisRS domain (and thus likely to be tRNA stimulated) but independent of amino acid starvation during growth of the cells (35). Thus, our results do not rule out the possibility that dimerization of GCN2 in vivo is triggered by the accumulation of uncharged tRNA (Fig. 9A).

Implications of interdomain interactions for regulation of GCN2 kinase activity. In addition to its role in dimerization and ribosome binding, the C-term domain appears to have additional functions in GCN2 kinase activation, as the most potent *GCN2*^{c} activating mutations were isolated in this region (7, 25, 32). Accordingly, the physical interaction that we detected between the C-term and PK domains could be related to a regulatory function. One interesting possibility depicted in Fig. 9 is that the C-term domain has an autoinhibitory function, binding in the vicinity of the active site to interfere with dimerization, substrate binding, or catalysis by the PK domain under nonstarvation conditions, where GCN2 is inactive. Although the pairwise interactions between the isolated C-term and PK domains were weak, as judged by in vitro binding reactions with GST fusion proteins, these interactions might be stabilized by a combination of the much stronger PK-HisRS and HisRS–C-term domain intramolecular interactions that we detected (Fig. 3). If the C-term segment has an autoinhibitory function, one may predict that its removal will produce constitutive activation of GCN2, whereas deletions in this region abolish *GCN2* function in vivo (24, 32) (Table 3). However, such deletions may also impair dimerization or ribosome binding by GCN2 in addition to removing the putative inhibitory function of the C-term domain.

The isolated ψPK and HisRS regions each interacted strongly with the PK domain of GCN2, and the HisRS domain also showed strong binding to the C-term region in our in vitro assays. These interdomain interactions involve adjacent segments in GCN2, and it is possible that they primarily reflect contacts at the domain interfaces which give GCN2 a compact structure. Alternatively, the strong PK-ψPK and PK-HisRS interactions may also contribute to negative regulation of the PK domain under nonstarvation conditions, as depicted in Fig. 9. Because high-level phosphorylation of eIF2 by GCN2 inhibits total protein synthesis (25), it may be necessary to have redundant means of inhibiting the PK domain to provide a fail-safe mechanism for activating GCN2 function. As suggested above, the PK-ψPK and PK-HisRS interactions could also have a role in blocking dimerization of the PK domain in nonstarved cells. The effects of insertion and deletion mutations in the HisRS and ψPK domains indicate that these regions have a positive role in activating GCN2 in starved cells (31, 32, 35). As suggested for the C-term segment, however, the ψPK and HisRS segments may play both positive and negative roles in GCN2 regulation.

In the hypothetical model shown in Fig. 9A, we suggest that interactions of the PK domain with the C-term, HisRS, and ψPK regions all contribute to the inactivity of GCN2 under nonstarvation conditions by preventing dimerization, blocking autophosphorylation, and interfering with proper binding of the substrate to the active site. Binding of uncharged tRNA to the HisRS region would trigger a conformational change that replaces these inhibitory interdomain interactions with self-

interactions that stabilize GCN2 dimer formation. *trans*-Autophosphorylation would occur in the dimer, followed by binding and phosphorylation of the substrate eIF2. We recently presented evidence that autophosphorylation of Thr residues 882 and 887 between subdomains VII and VIII, the so-called activation loop of the PK domain, is required for GCN2 kinase function (26). In the alternative model shown in Fig. 9B, both the inactive and the active forms of GCN2 exist as dimers, and the interdomain interactions are responsible for preventing autophosphorylation and eIF2 binding. As in Fig. 9A, a conformational change would accompany the binding of uncharged tRNA, releasing the PK domain from multiple inhibitory interactions with the adjacent regulatory domains. Proving an autoinhibitory function of the C-term segment and the roles of other domain interactions in regulating GCN2 kinase function will require the isolation of point mutations that disrupt each interaction and then determining the effect of such mutations on GCN2 catalytic function and its regulation by uncharged tRNA.

ACKNOWLEDGMENTS

We thank Cuihua Hu for excellent technical assistance, Clyde Denis for anti-LexA antibodies, Tom Dever for helpful comments on the manuscript, and Bobbie Felix for help in manuscript preparation.

REFERENCES

1. **Bardwell, L., A. J. Cooper, and E. C. Friedberg.** 1992. Stable and specific association between the yeast recombination and DNA repair proteins RAD1 and RAD10 in vitro. Mol. Cell. Biol. **12:**3041–3049.
2. **Boeke, J. D., F. LaCroute, and G. R. Fink.** 1984. A positive selection for mutants lacking orotidine-5′-phosphate decarboxylase activity in yeast: 5-fluoro-orotic acid resistance. Mol. Gen. Genet. **197:**345–346.
3. **Bradford, M. M.** 1976. A rapid and sensitive method for the quantitation of microgram quantities of protein utilizing the principle of protein-dye binding. Anal. Biochem. **72:**248–254.
4. **Cesareni, G., and J. A. H. Murray.** 1987. Plasmid vectors carrying the replication origin of filamentous single-stranded phages, p. 135–154. *In* J. K. Setlow and A. Hollaender (ed.), Genetic engineering: principles and methods, vol. 9. Plenum Press, New York, N.Y.
5. **Cusack, S., M. Hartlein, and R. Leberman.** 1991. Sequence, structural and evolutionary relationships between class 2 aminoacyl-tRNA synthetases. Nucleic Acids Res. **19:**3489–3498.

5a. **Dever, T.** Personal communication.

6. **Dever, T. E., L. Feng, R. C. Wek, A. M. Cigan, T. D. Donahue, and A. G. Hinnebusch.** 1992. Phosphorylation of initiation factor 2α by protein kinase GCN2 mediates gene-specific translational control of *GCN4* in yeast. Cell **68:**585–596.
7. **Diallinas, G., and G. Thireos.** 1994. Genetic and biochemical evidence for yeast GCN2 protein kinase polymerization. Gene **143:**21–27.
8. **Driscoll-Penn, M., G. Thireos, and H. Greer.** 1984. Temporal analysis of general control of amino acid biosynthesis in *Saccharomyces cerevisiae*: role of positive regulatory genes in initiation and maintenance of mRNA derepression. Mol. Cell. Biol. **4:**520–528.

8a. **Garcia-Barrio, M. T., and A. G. Hinnebusch.** Unpublished observations.

9. **Gietz, R. D., A. R. Willems, and R. A. Woods.** 1995. Studies on the transformation of intact yeast cells by the LiAc/SS-DNA/PEG procedure. Yeast **11:** 355–360.
10. **Golemis, E. A., J. Gyuris, and R. Brent.** 1996. Interaction trap/two-hybrid system to identify interacting proteins, p. 20.1.1–20.1.28. *In* F. M. Ausubel, R. Brent, R. E. Kingston, D. D. Moore, J. G. Seidman, J. A. Smith, and K. Struhl (ed.), Current protocols in molecular biology. John Wiley & Sons, Inc., New York, N.Y.
11. **Gyuris, J., E. Golemis, H. Chertkov, and R. Brent.** 1993. Cdi1, a human G1 and S phase protein phosphatase that associates with Cdk2. Cell **75:**791–803.
12. **Hanks, S. K., and T. Hunter.** 1995. The eukaryotic protein kinase superfamily, p. 7–47. *In* G. Hardie and S. Hanks (ed.), The protein kinase facts book. Academic Press, Inc., San Diego, Calif.
13. **Heldin, C.-H.** 1995. Dimerization of cell surface receptors in signal transduction. Cell **80:**213–223.
14. **Hershey, J. W. B.** 1991. Translational control in mammalian cells. Annu. Rev. Biochem. **60:**717–755.
15. **Hinnebusch, A. G.** 1994. The eIF-2α kinases: regulators of protein synthesis in starvation and stress. Cell Biol. **5:**417–426.
16. **Hinnebusch, A. G.** 1996. Translational control of *GCN4*: gene-specific regulation by phosphorylation of eIF2, p. 199–244. *In* J. W. B. Hershey, M. B. Mathews, and N. Sonenberg (ed.), Translational control. Cold Spring Harbor Laboratory Press, Cold Spring Harbor, N.Y.

16a. **Kozak, M.** 1983. Comparison of initiation of protein synthesis in procaryotes, eucaryotes, and organelles. Microbiol. Rev. **47:**1–45.

17. **Laemmli, U. K.** 1970. Cleavage of structural proteins during the assembly of the head of bacteriophage T4. Nature **227:**680–685.
18. **Lanker, S., J. L. Bushman, A. G. Hinnebusch, H. Trachsel, and P. P. Mueller.** 1992. Autoregulation of the yeast lysyl-tRNA synthetase gene *GCD5*/*KRS1* by translational and transcriptional control mechanisms. Cell **70:**647–657.
19. **Lucchini, G., A. G. Hinnebusch, C. Chen, and G. R. Fink.** 1984. Positive regulatory interactions of the *HIS4* gene of *Saccharomyces cerevisiae*. Mol. Cell. Biol. **4:**1326–1333.
20. **Marton, M. J., C. R. Vazquez de Aldana, H. Qiu, K. Chakraburtty, and A. G. Hinnebusch.** 1997. Evidence that GCN1 and GCN20, translational regulators of *GCN4*, function on elongating ribosomes in activation of the eIF2α kinase GCN2. Mol. Cell. Biol. **17:**4474–4489.
21. **Mathews, M. B.** 1993. Viral evasion of cellular defense mechanisms: regulation of the protein kinase DAI by RNA effectors. Semin. Virol. **4:**247–257.
22. **Merrick, W. C., and J. W. B. Hershey.** 1996. The pathway and mechanism of eukaryotic protein synthesis, p. 31–69. *In* J. W. B. Hershey, M. B. Mathews, and N. Sonenberg (ed.), Translational control. Cold Spring Harbor Laboratory Press, Cold Spring Harbor, N.Y.
23. **Messenguy, F., and J. Delforge.** 1976. Role of transfer ribonucleic acids in the regulation of several biosynthesis in *Saccharomyces cerevisiae*. Eur. J. Biochem. **67:**335–339.

23a. **Pharmacia.** 1996. GST Gene Fusion System Manual. Pharmacia, Uppsala, Sweden.

23b. **Qiu, H., and A. G. Hinnebusch.** Unpublished observations.

24. **Ramirez, M., R. C. Wek, and A. G. Hinnebusch.** 1991. Ribosome association of GCN2 protein kinase, a translational activator of the *GCN4* gene of *Saccharomyces cerevisiae*. Mol. Cell. Biol. **11:**3027–3036.
25. **Ramirez, M., R. C. Wek, C. R. Vazquez de Aldana, B. M. Jackson, B. Freeman, and A. G. Hinnebusch.** 1992. Mutations activating the yeast eIF-2α kinase GCN2: isolation of alleles altering the domain related to histidyl-tRNA synthetases. Mol. Cell. Biol. **12:**5801–5815.
26. **Romano, P. R., M. T. Garcia-Barrio, X. Zhang, Q. Wang, D. R. Taylor, F. Zhang, C. Herring, M. B. Mathews, J. Qin, and A. G. Hinnebusch.** 1998. Autophosphorylation in the activation loop is required for full kinase activity in vivo of human and yeast eukaryotic initiation factor 2α kinases PKR and GCN2. Mol. Cell. Biol. **18:**2282–2297.
27. **Schnarr, M., M. Granger-Schnarr, S. Hurstel, and J. Pouyet.** 1988. The carboxy terminal domain of the LexA repressor oligomerises essentially as the entire protein. FEBS Lett. **234:**56–60.
28. **Sherman, F., G. R. Fink, and C. W. Lawrence.** 1974. Methods of yeast genetics. Cold Spring Harbor Laboratory, Cold Spring Harbor, N.Y.
29. **Towbin, H., T. Staehelin, and J. Gordon.** 1979. Electrophoretic transfer of proteins from polyacrylamide gels to nitrocellulose sheets: procedure and some applications. Proc. Natl. Acad. Sci. USA **76:**4350–4354.
30. **Vazquez de Aldana, C. R., R. C. Wek, P. San Segundo, A. G. Truesdell, and A. G. Hinnebusch.** 1994. Multicopy tRNA genes functionally suppress mutations in yeast eIF-2α kinase GCN2: evidence for separate pathways coupling *GCN4* expression to uncharged tRNA. Mol. Cell. Biol. **14:**7920–7932.
31. **Wek, R. C., B. M. Jackson, and A. G. Hinnebusch.** 1989. Juxtaposition of domains homologous to protein kinases and histidyl-tRNA synthetases in GCN2 protein suggests a mechanism for coupling *GCN4* expression to amino acid availability. Proc. Natl. Acad. Sci. USA **86:**4579–4583.
32. **Wek, R. C., M. Ramirez, B. M. Jackson, and A. G. Hinnebusch.** 1990. Identification of positive-acting domains in GCN2 protein kinase required for translational activation of *GCN4* expression. Mol. Cell. Biol. **10:**2820–2831.
33. **Wek, S. A., S. Zhu, and R. C. Wek.** 1995. The histidyl-tRNA synthetase-related sequence in the eIF-2α protein kinase GCN2 interacts with tRNA and is required for activation in response to starvation for different amino acids. Mol. Cell. Biol. **15:**4497–4506.
34. **Zhang, F., M. Kirouac, N. Zhu, A. G. Hinnebusch, and R. J. Rolfes.** 1997. Evidence that complex formation by Bas1p and Bas2p (Pho2p) unmasks the activation function of Bas1p in an adenine-repressible step of *ADE* gene transcription. Mol. Cell. Biol. **17:**3272–3283.
35. **Zhu, S., A. Y. Sobolev, and R. C. Wek.** 1996. Histidyl-tRNA synthetase-related sequences in GCN2 protein kinase regulate *in vitro* phosphorylation of eIF-2. J. Biol. Chem. **271:**24989–24994.